Temporal and spatial receptive field characteristics of tectal neurons in zebrafish larvae

1. Gutachter: Prof Tobias Bonhoeffer (Vorsitz der Pruefung)

2. Gutachter: Prof . Benedikt Grothe

3. Pruefer: Prof. Rainer Uhl

4. Pruefer: Prof. Sebastian Diehl (Protokoll)

Tag der mündlichen Prüfung: 21.3.2006

CONTENTS

1   SUMMARY

Understanding the neuronal coding mechanisms with which neurons in the central visual system process their inputs is the main goal of this thesis. Neurons in the visual system of zebrafish larvae process information about the visual world only in a restricted window of space and time. Their so called spatio-temporal receptive fields were of central interest to this study. They were measured with in vivo patch clamp recordings and are described in detail for cells in the neuropil of the larval optic tectum.

The temporal receptive fields (or moments) were calculated with reverse correlation of a whole field Gaussian white noise flicker stimulus with the current traces that were evoked by this stimulus sequence. Temporal moments can be either monophasic, that is pure 'on' or 'off', or multiphasic (a combination of 'on' and 'off' components). During the first week of development, the dominance of 'off' moments observed for the youngest animals (3-4 days post fertilization, dpf) changes to more common 'on' moments for animals of 10-11 dpf. For the whole group of 3-11 days 44.9% of all cells had a biphasic moment. The percentage of biphasic cells increases significantly from younger to older cells which is consistent with the temporal maturation observed in other vertebrates (Cai et al., 1997).

The spatial extend of the receptive fields was determined to a mean of 17 degrees (+/-10) for an 'off' stimulus and 14 (+/-10) for the 'on' stimulus. No spatial refinement was observed to take place within the period of 3-11 dpf. This is surprising considering the massive morphological rearrangement that is taking place during hat time at the retino-tectal connection (Gnuegge et al., 2001) but consistent with a study of a different class of larval zebrafish tectum neurons, the periventricular zone (PVZ) cells (Niell and Smith, 2005). The receptive fields of neuropil cells are not retinotopically organized.

20 neurons were tested for motion sensitivity and all of them were found to respond equally well or better to moving stimuli than stationary dots of comparable size. Some cells showed non-linear spatial summing, that is they responded with a larger current to small spots than to big spots. Direction selectivity was not observed, but a preference for one orientation of movement could be seen often (12 out of 20 cells).

In the second part of the thesis, the information about receptive field properties was used in a linear model to predict responses to a new stimulus. This approach of comparing measured and modeled data is widely used to test the understanding of neuronal coding mechanisms (for example (Keat et al., 2001). How well the model matches the data is a direct measurement of how comprehensive it is.

The stimuli that were chosen for the prediction study were a series of different natural movies and simulated natural-like movies. 30 neurons could be recorded (voltage clamp) that responded reproducibly to several repetitions of a given movie which is a crucial condition in order to achieve a reasonable prediction match. 8 most reliable cells were attempted to be predicted and for all of those the prediction algorithm was able to perform well with respect to event occurrence and duration. The exact amplitude of the responses did not always match which can be explained by several non-linear characteristics the cells display.

This study is a first approach of understanding the visual processing of neurons in the central visual system with the means of in vivo voltage clamp recordings together with modeling attempts of a natural stimulus and has led to a vast of insight into the input output functions of the studied cells.

2   INTRODUCTION

Sensory systems receive, encode, and transmit information about the outer world to areas of the brain that process this information and transform it into an output that results in an appropriate behavior. Understanding the rules governing information encoding in neuronal signals has been a central goal for decades of research in neuroscience.

In this thesis, the encoding properties of neurons in the visual system of zebrafish are investigated by measuring neuronal responses to a visual stimulus that results in a prey capture behavior and comparing the measured responses to modeled responses. The quality of how the model fits the data can be used as a direct measurement of our understanding of the coding mechanisms of this system.

2.1   THE VISUAL SYSTEM IN ZEBRAFISH AND VISUALLY INDUCED BEHAVIOR

Zebrafish have become an established vertebrate model system in many areas of research, including neurobiology. The larval zebrafish is already a well established model system for studying development of the visual system and visual behavior but only few studies have focused on the functional properties of neurons in the visual system downstream of the retina in both, larval and adult zebrafish. The animal is extremely well suited for functional investigation of the visual system for several reasons. After fertilization, the eggs develop into freely moving larvae that display a variety of visually guided behaviors within a few days (Easter, Jr. and Nicola, 1996). One of the more interesting behaviors at this age is prey capture which is crucial for the animal to survive as the yolk is slowly degrading at this point and the animal needs to feed from outside sources, such as paramecia. zebrafish larvae use their vision to hunt for food as early as 4 days post fertilization (dpf). To hunt, the fish orient their eyes after moving objects and quickly dart forward to swallow one. The eye movement that precedes the prey capture and the observation that larvae don't hunt in the dark, indicate a strong involvement of the visual system in this behavior. Deletion studies have shown that it is very likely that neurons that are involved in

generating this behavior lie within the optic tectum (Gahtan et al., 2005). In the last decade the zebrafish has become a very popular vertebrate genetic model system and several studies have identified mutants with deficits in the visual system (Karlstrom et al., 1996a). Many tools are readily available to dissect and investigate the function of different genes with respect to anatomy, physiology, and visually guided behavior (Guo, 2004;Orger et al., 2004;Vogel, 2000).

The visual system of all vertebrates consists basically of the retina where light transduction and signal preprocessing takes place, an optic nerve that conveys the information to the brain, and several areas in the brain where neuronal signals are relayed and furthermore processed. In the retina, the detection of light by the photoreceptors leads via several interneurons to the activation of ganglion cells (RGCs) which serve as the output layer of the retina and project to the brain.

In the zebrafish larvae the main projection site of RGC axons is the contralateral optic tectum (OT), the visual midbrain. The axons of the ganglion cells project to the tectum retinotopically along the rostro-caudal axis, resulting in axons from temporal RGCs terminating further rostrally than axons from cells in the nasal retina. Figure 1 shows the zebrafish, concentrating on the visual brain structures.
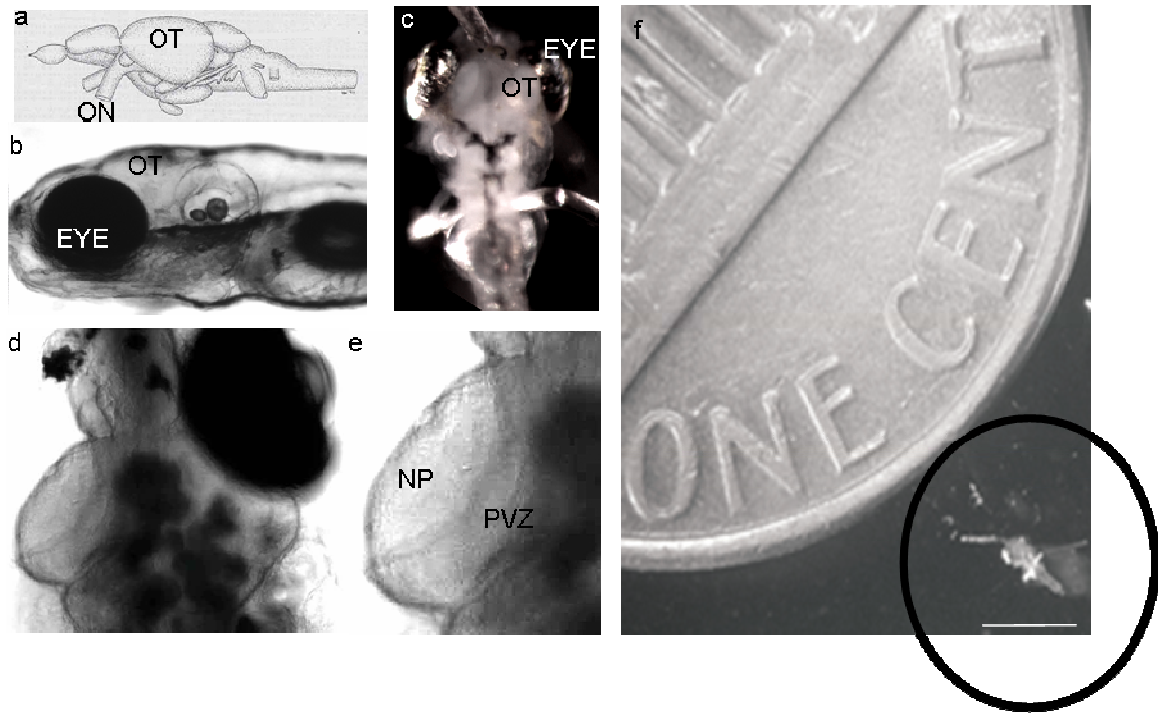
Figure 1: The visual system of zebrafish
a: schematic saggittal drawing of an adult zebrafish brain (modified from (Wullimann et al., 1996)), b: zebrafish larvae oriented the same way as in a, c: open brain preparation of larval zebrafish, dorsal view. The animal is fixed with insect pins. d: close up of the exposed tectum with the ipsilateral eye removed. e: zoom in on the tectum, marked is the lateral neuropil and the medial PVZ (periventricular zone). OT=optic tectum, ON=optic nerve, NP=neuropil. f: scale bar. image in c in relation to a US 1 cent coin., white scale bar=2mm.

The OT consists of about 300000 (partly counted and estimated in the lab) neurons and is therefore a relatively simplified visual pathway that allows for detailed investigation of central visual neurons. It is a very prominent structure in the larval fish brain which lies dorsal behind the eyes and covers about half the length of the whole brain. The third ventricle is surrounded by the caudal part of the two tectal hemispheres. Within the OT one can distinguish primarily between two obvious anatomical structures: the medial periventricular grey zone (PVZ) which holds about 90% of all cell bodies extends many layers down to the ventral areas of the brain and the dorsolateral neuropil which is the entry site of the RGC axons and holds mostly processes and very few cell bodies that lie very superficial in one or two sparse layers. PVZ cells continue to have the same functional organization as the RGCs with regard to representation of location in space (retinotopy)

9

(Niell and Smith, 2005). Neurons in the PVZ send numerous dendritic projections into the neuropil. Typically the dendrites of PVZ neurons enter the neuropil parallel to each other, resulting in a ladder-like structure running perpendicular to the rostro-caudal axis of the brain (Niell et al., 2004). This spatially organized layout could be a morphological basis underlying the upkeep of retinotopy. The morphology of larval neuropil cells displays a generally different organization than PVZ cells. Neurons in the neuropil have largely elongated dendritic trees that can span up to half the rostro caudal axis. Generally, a combination of all adult cell classes can be found in the neuropil at around 7dpf (Naumann E.A. and Engert F., 2005). The dendrites span over such a large area of the tectum that they could receive inputs from many different parts of the retina. It can be speculated that this large dendritic integration area might be responsible for the lack of retinotopy within these cells (see results).

At this age, the larvae have not yet developed a solid skull and so the only tissue covering the brain is the outer skin and the meninges which makes the brain optically very accessible. The softness of the early skin also allows for relatively easy surgery to expose the brain and make it accessible for electrophysiological recordings with micro pipettes, both extracellular and intracellular.

It is feasible to record from a large number of neuropil neurons intracellularly in many different animals since virtually all of the cells in the neuropil are light responsive, the surgery to expose the cells is uncomplicated, and the young animals stay alive for several hours without further effort (e.g. no perfusion of the gills or of the recording chamber is needed).

The electrophysiological accessibility together with a behaviorally relevant stimulus makes this system extremely powerful to study encoding mechanisms in the visual system. Furthermore, different mutants with changes in the visual system have been identified that can be used to dissect the role of different genes for certain visual behaviors.

2.2   INFORMATION CODING IN NEURONAL SIGNALS

Visual encoding begins in the retina where graded potential changes of receptor neurons and interneurons lead to an all or none transmission in ganglion cells. Beyond the retina, the only information about visual stimuli available to the brain is binary in the form of spike trains. Spikes arriving at any given postsynaptic cell will be integrated within that cell and if the integrated currents are large enough to cross firing threshold, the cell will fire spikes onto other target cells. The information carried in spike trains can be encoded in the number of spikes, the frequency, and the overall length of ongoing signals. Since the output of central neurons occurs in this all or nothing manner, recoding can occur at every neuron. It might affect any parameter of the spike train such as for example frequency or number of spikes. All the previously integrated inputs are reshaped into different spike trains before they are communicated to downstream cells in a circuit. This process of input integration and threshold spike generation facilitates the transmission of information to higher levels of the brain where neuronal codes become more and more comprehensive.

At all instances, each postsynaptic cell functions as a read out detector that has limited access to what information was available to upstream encoders. An experimental method to access neuronal signals is the technique of patch-clamp recordings. Microelectrodes filled with saline solution that resembles the concentration of ions inside a neuron can be used in current clamp configuration to record excitatory postsynaptic potentials (EPSPs) and action potentials or in voltage clamp configuration to obtain recordings of excitatory postsynaptic currents (EPSCs).

In this thesis, sub-threshold currents are recorded from cells in the optic tectum that receive direct inputs from the retina and probably also from intertectal connections.

2.3   MEASURING VISUAL ENCODING PROPERTIES

To understand how visual information is encoded into neuronal responses and decoded by downstream neurons, it can be helpful to model the stimulus/response transformation or input/output relationship of a neuron.

An established approach to determine an input/output function for spike trains is the reverse correlation technique. The so called first moment (or kernel) can be described as a linear filter for a given cell and it is obtained by cross correlating the data (e.g. spike train or current trace) with a stimulus waveform. It is a quantitative and generally valid description of a cell with respect to the chosen dimensions and within the limits of linear components (de Boer and Kuyper, 1968).

The stimulus however, needs to be chosen carefully to avoid introducing any bias into the filters one wishes to obtain. The least biased stimulus is pure Gaussian white noise shown at a sufficiently high update rate to avoid under sampling of the cell's frequency response capability, in both spatial and temporal domain. The simplest way of utilizing linear Gaussian white noise (LGWN) to measure the moment of a cell, is to use a one dimensional noise stimulus. The whole visual area is illuminated with a fast flickering of linearly dependant light intensities. This can for example be achieved by feeding different voltages into a light emitting diode (LED) that will result in different light intensities.

In a linear system, the moment can be applied to predict the responses to other stimuli of the same dimension: convolution of the moment with a given (new) stimulus waveform yields the predicted responses of the cell to that stimulus.

The visual system is specialized to detect different objects within different areas of the whole visual field and therefore a one dimensional description is far from complete. Two dimensional stimuli need to be used to describe the cell's spatial receptive field (RF). It can be regarded as a linear filter that delineates the region of visual space a cell is responsive to. Inside this area the cell's preference can be limited to either an increase or a decrease of the light intensity ('on' cell/'off' cell) or a combination of both ('on-off', center-surround). The preference for 'on' and 'off' areas can be homogeneous for the entire receptive field or different for respective sub-areas within the RF. In the vertebrate visual system a vast variety of receptive fields have been described for different cells and in

different animals (Bair, 2005;Cai et al., 1997;DeAngelis et al., 1995;Hubel and Wiesel, 1959;Mancini et al., 1990;Martinez et al., 2005;Mechler and Ringach, 2002;Van Hooser et al., 2003). Typically, receptive fields of retinal ganglion cells have a center surround structure, where the best activation of the cells occurs when one area is illuminated while the other area is in the dark. Further downstream in the visual pathway receptive fields can have a distinct geometrical structure, such as simple cells in mammalian V1 that are best driven by bars, or can be astonishingly specific to features such as face cells in IT of primates that respond preferentially when presented with an image of a face (Bruce et al., 1981). It is obvious thus, that many receptive field properties are highly non-linear and one has to accommodate for that when choosing a stimulus to probe different cells. A two dimensional Gaussian white noise stimulus is suitable and at least theoretically the stimulus of choice to describe a cell's receptive field comprehensively and in an unbiased way. The two dimensional GWN stimulus contains all spatial and temporal frequencies and will therefore probe the cell's response properties extensively when presented long enough. However, experimentally all in vivo recordings are time limited and may not allow for collecting enough data to obtain meaningful multi dimensional receptive fields with reverse correlation of a two dimensional Gaussian white noise stimulus. Determining beforehand, which stimulus parameters will be irrelevant for the investigated system and eliminating those from the white noise can reduce the necessary recording time dramatically. The most commonly used complex stimuli are pseudorandom stimuli such as sparse noise (Jones and Palmer, 1987), white noise (Reid et al., 1997), and dynamic gratings (Mechler and Ringach, 2002). A comparison of necessary stimulation time with different stimuli is shown in Figure 2. For this figure a simulated receptive field of a linear model cell is assumed. The receptive field is convoluted with the respective stimulus to obtain the simulated responses that would have led to the RF. The response time that would have been needed to calculate the simulated receptive field and how well it would be approximated is shown in Figure 2 for white noise (black), filtered white noise (blue) and a checkerboard stimulus of comparable resolution like the filtered noise (red). The filtered noise is obtained by deleting irrelevant spatial frequencies from the stimulus in the Fourier spectrum (see Figure 2 and methods). The simulated receptive field can be

calculated fastest and to a best approximation with the filtered noise stimulus or the checkerboard.
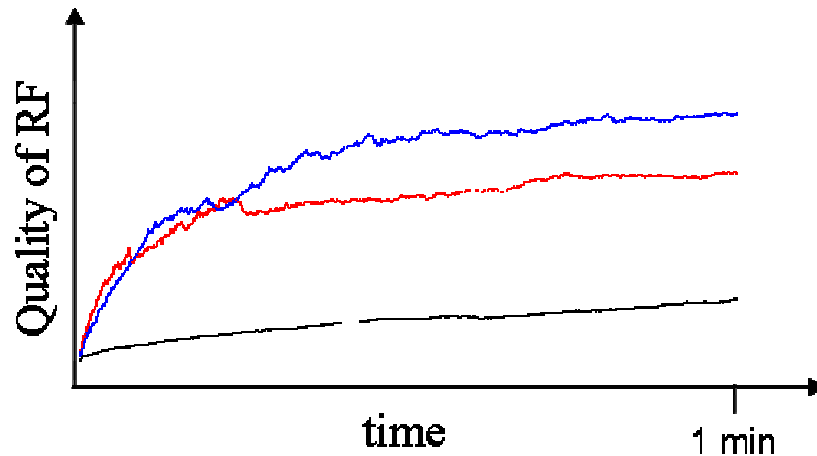

Figure 2: Measuring receptive fields with different methods yields different qualities of RF
The blue, red and black graph reveal the different amount of time it takes to measure a simulated field. The Y-axis displays the relative quality of the receptive field. Black: calculation with white noise, blue: with filtered noise, red: with a checkerboard of comparable resolution as the filtered noise. Note that initially both, filtered noise and checkerboard result in an equally satisfying receptive field approximation, whereas the white noise measurement increases the quality of the measurement only with a very flat slope.

The resulting filtered noise might however introduce a bias into the measurement, depending on how much is was filtered. The same is true for measurements with checkerboard stimuli that can only resolve receptive fields up to the resolution of the size of one square. Extensive preliminary experiments need to be done to exclude stimulus parameters. Figure 3 explains how the spatial noise stimulus is filtered. Extracting specific frequencies out of a high dimensional noise stimulus requires the Fourier transformation which yields all the components of the stimulus in frequency space (middle panel in Figure 3). Frequencies are aligned in increasing order from the middle to the outside of the spectrum. All frequencies one wants to eliminate can be cut out of the spectrum; in this case it was chosen to cut out only the highest (outside) frequencies. The inverse Fourier transform results in the shaped noise in stimulus space which is shown to the fish. Preliminary experiments were done to determine the cut-off frequency.

14

Low/high resolution   Fourier transform (FFT)   Cut out   Inverse Fourier transform
2-dimensional white noise   of white noise   high frequencies
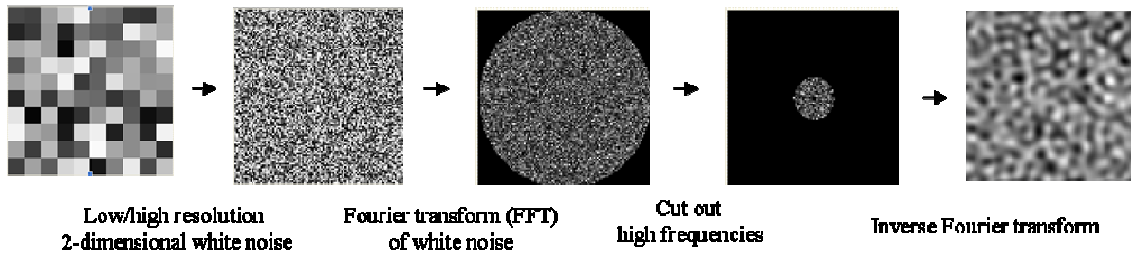
Figure 3: White noise and filtered noise
A helpful approach to limit the necessary recording time to measure a spatio-temporal receptive field with one stimulus is to filter the frequency spectrum of a high resolution noise. Cutting out any frequencies (here only the highest) requires a Fourier transformation (FFT) which yields the complete frequency spectrum of the stimulus. The frequency bandwidth that can be eliminated has to be estimated empirically. The inverse FFT will result in a shaped noise stimulus that is lacking all unwanted frequencies.

It is of course crucial, that the frequency spectrum of the measured receptive field is contained within the stimulus. If one isn't sure whether that's the case, it is strongly advisable to increase the frequency spectrum of the stimulus and measure the same RF again. An example for a receptive field measured with a sufficient frequency spectrum and another one where the frequency spectrum of the stimulus was not broad enough is shown in Figure 4. The white pixels display frequencies contained within each spectrum. In a, the receptive field spectrum is smaller than that of the used stimulus which means that the stimulus was suitable to measure this receptive field and no necessary frequencies were left out. In b however, the frequency spectra of both highly overlap. One can assume here that more spatial frequencies in the stimulus would result in a different (smaller) receptive field that was not resolvable with the applied stimulus; the resolution was not high enough. Another way of testing parameters of a cell that are relevant without having to record for too long is to split the stimuli and test for one or more features in every dimension.

receptive field   stimulus

a

b
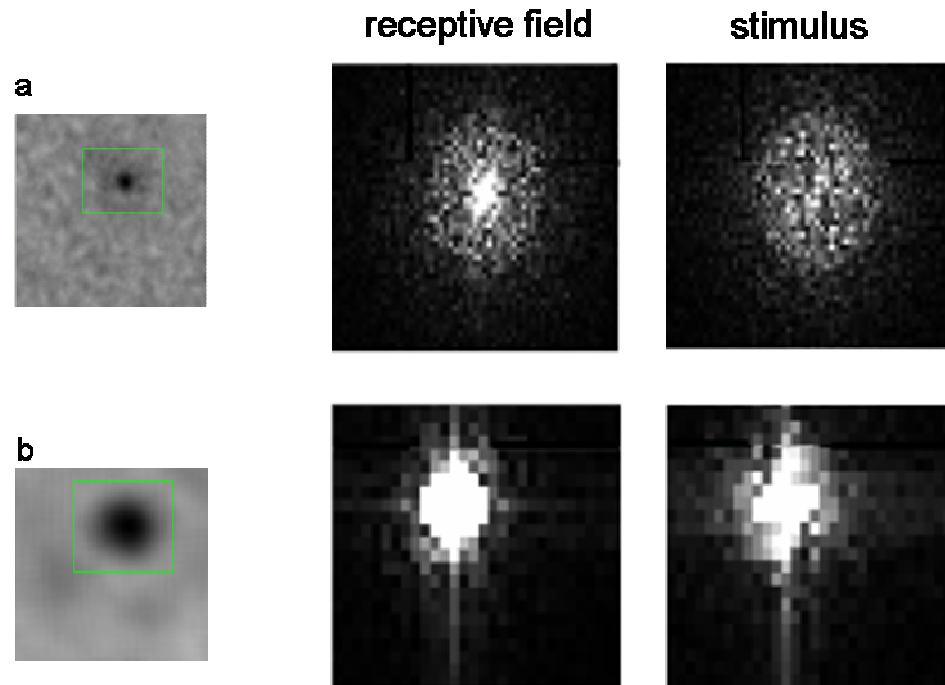
Figure 4: Frequency spectra of 2 receptive fields and stimuli
a: left: receptive field, right: frequency spectrum of receptive field and stimulus respectively. The frequency spectrum of the receptive field is contained within that of the stimulus. b: same as in a but here the frequency spectra mostly overlap which indicates that the stimulus was not suited to measure this RF.

One can define the spatial extend of the receptive field with conventional methods by flashing reasonably sized spots within the visual field and, if necessary, raise the resolution once a coarse receptive field area has been determined. Together with a one dimensional moment this approach can give good insight into the cells encoding properties, given that it functions mostly linear. An advantage of this combined approach is that a comprehensive spatial and temporal description can be obtained in only a few minutes.

However, most cells in the visual system do not process information in a purely linear way. In fact, most of the interesting processing capabilities of the brain will have to arise from non-linear interactions. Several nonlinearities in signal processing can be observed and have been described extensively. Technically these could in theory be accounted for by a real "endless" Gaussian white noise stimulus, less so by the filtered noise but not at all when the receptive field is measured statically by flashing dots.

Results from the literature together with preliminary experiments in the lab were used to conclude which stimuli were sensible to test for and which stimuli could be ignored because they were not driving the cells.

The individual testing of different linear and non-linear properties might seem laborious. One has to test a large variety of stimuli on an even bigger population of cells to obtain an overview for possible stimuli that need to be tested in order to understand neuronal response properties comprehensively. However, if one faces practical limitations that make long measurements with two dimensional white noise unfeasible, a similar insight for a population of cells can be gained with the individual experiments. One assumption that has to be made however, is that all cells within one investigated group show roughly similar characteristics. One can then specify boundary conditions from a large set of cells and develop a stimulus protocol that encloses all the beforehand determined stimuli that should be presented to a final set of cells.

If the experimental situation allows for recordings of many cells for a limited time rather than few cells for very long, this combinatorial approach is a possible way of describing coding properties of cells. One first creates a framework with population data that can then be transferred to a final set of cells. The final stimulus protocol will consist of a combination of the 'best' tested stimuli.

2.4   MODELING VISUAL RESPONSE PROPERTIES

Experimental recordings of neuronal response properties to different visual stimuli can be used to fit parameters for a model. The validity of a model can then be tested by attempting to predict the neuronal responses to a novel stimulus.

Historically, models of visual encodings are based on the concept of a spatial receptive field and they can be dramatically improved by adding the concept of a temporal receptive field such as the temporal moment. Understanding neuronal encoding characteristics with receptive field based models has been successful in several sensory systems; however, problematic assumptions have had to be made.

The visual system is highly specialized to detect changes in the environment, for example moving objects and changes in light intensity. In spite of this, the estimation of its

17

encoding properties is often attempted with static parameters such as the stationary receptive field. Some approaches to describe the receptive field concentrate on the spatial receptive field properties only, without taking into account temporal dynamics that may be necessary to describe the neural properties in full. Other approaches lose temporal information by having to average over many trials of stimulus presentation within the RF. Only when the temporal response characteristics of the neuron are independent of the spatial position of the stimulus (space time separable RF) can it be meaningful to obtain a RF in this static manner. One still has to define temporal RF properties of the cell but this can de done independently. For cells with space time inseparable receptive fields it is crucial to combine space and time measurements to be able to describe the cell correctly. For the neurons described in this study, the space time separability was tested thoroughly with a series of two dimensional spatially filtered noise experiments (see results).

To model neuronal responses to dynamic stimuli, such as natural scenes, one has to take into account the spatio-temporal interactions of a system to describe it adequately.

A general challenge for describing neuronal response properties with a linear model seems to be the problem of accommodating several non-linearities within that model. Specific nonlinear responses characteristics can be observed beforehand and then added separately into the model. Figure 5 illustrates the linear model with a rectifying non-linearity added that is used in this study. A stimulus, in this case a movie of paramecia, is convolved with both, the temporal and spatial receptive field filters. To this extend, each frame of the movie is multiplied with the receptive field properties and averaged. A rectifying non-linearity is added to ensure that only excitatory responses (inward currents) will be predicted. This is necessary because cells were held at a holding potential around -55 to -60 mV where usually all positive charges flow into the cell.

A failure to accommodate for widely occurring nonlinear characteristics will result in failing predictions wherein for example the timing of the onset of events fits the data accurately but the single events are under- or overestimated in their amplitude and/or duration. The addition of specific non-linearities into the receptive field model, for example a motion preference can be useful to avoid over- or under-predicting responses that a linear model is incapable of accounting for correctly. Another, computationally much more challenging possibility is to use a neural network to model the responses. Few

assumptions have to be made in order for a network to converge onto a satisfying fit after recurring alterations of initially set parameters.
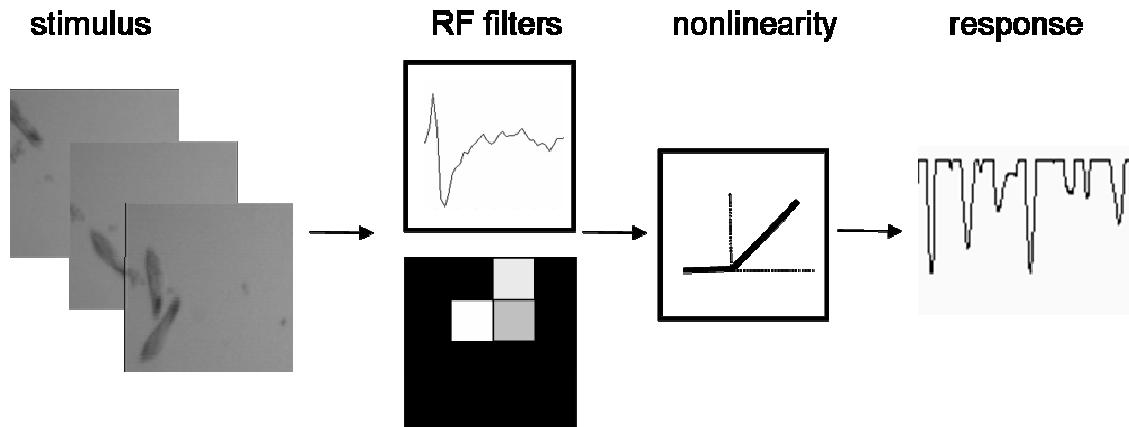

Figure 5: Linear-nonlinear modeling
A novel stimulus is convoluted with the available receptive field properties, in this case spatial and temporal and a nonlinearity (rectifier) is added to compute the responses.

White noise analysis should account for detecting most non-linearities when applied appropriately and it has been successfully used in a wide variety of preparations to characterize the input-output behavior of linear and non-linear systems for many different modalities (Chichilnisky, 2001) but some experimental disadvantages of pure white noise techniques such as the long necessary recording times have been illustrated above.

So far, several successful efforts can be found in the literature to describe neuronal coding properties and evaluation of the quality of the description by comparing predicted neuronal responses to measured data (Keat et al., 2001;Touryan et al., 2005).

However, most prediction studies up to date have been limited to using stimuli that are far less complex in their spatio-temporal content than the studied system, usually the vertebrate visual system, is capable of processing (Keat et al., 2001). Alternatively, in a study where natural stimuli were included, they were not only used to test a prediction algorithm but also to obtain certain parameters of the cells, for example the orientation tuning (Touryan et al., 2005). It is yet an unsolved challenge to understand neuronal coding of behaviorally relevant, natural scenes in a complete and super-awesome mathematically satisfying way by measuring their linear properties.

A common restriction for all modeling approaches is that the chosen system has to guarantee a certain response invariability across repeated presentations of the same stimulus in order to give a model a fair chance in predicting the responses well. Most modeling attempts so far are made by predicting spike trains of cells in the early visual system that process information about the visual world within a localized region of space, and a restricted period of time. More importantly, these neurons have a high response reliability across repeated trials (Berry et al., 1997;Berry and Meister, 1998), (Kara et al., 2000). Neurons in the zebrafish optic tectum process visual stimuli with a remarkable response invariability at the level of sub threshold currents. Repetitions of the same stimulus produce nearly identical response traces (see Results, (Figure 30)).

2.5   STRUCTURE OF THE THESIS

How information is encoded by neuronal responses has been a challenging question for several decades. In particular the problem of how encoding mechanisms govern processing of natural stimuli in the brain is still unsolved.

Characterizing a neuron's response to a given set of stimuli is a first step towards understanding how the cell encodes its inputs. Furthermore, one can use this knowledge to model the responses to a new stimulus. Predicting successfully how this neuron will respond to any other new stimulus is a comprehensive and concise description of a given neuron's coding mechanisms.

In the first part of this thesis, a comprehensive set of visual stimuli is used to describe response properties of neurons in the optic tectum of zebrafish larvae.

In the second part, the experimentally obtained information about neuronal response characteristics is used in a model to predict responses to a behaviorally relevant natural scene. The parameters for the model are specified by measuring the spatial and temporal receptive field characteristics with a combination of conventional and reverse correlation techniques. Additionally, several separate stimulus sequences are used to determine possible nonlinear properties of the cells. Different spatial model approaches have been used and are evaluated and discussed with the specific failures they display. Furthermore an evaluation of the best fitting algorithm is described for several cells. A comparison of the presented results with previously published works leads to a discussion of open questions and future directions.

Given the low response variability of neurons in the tectal neuropil and their accessibility for in vivo intracellular recordings, the larval zebrafish tectum provides the necessary physiological and experimental conditions to test predicted synaptic currents and compare them with the measured data. Space-time separability of the receptive fields allows for collecting spatial and temporal receptive fields separately. Application of reverse correlation is an unbiased method to describe the neuronal (here temporal) filter functions of a novel system. The availability of a behaviorally relevant natural stimulus allows for testing the system with an appropriate complexity. Sufficient recording time is

given to collect the data needed for measuring several nonlinear properties of the cell after establishing location and dynamics of the receptive fields.

Considering the above listed advantages, this system is a powerful model to evaluate our understanding of neuronal coding mechanisms that arises from measuring its linear spatio-temporal properties.

3 METHODS

3.1 FISH PREPARATION AND ELECTROPHYSIOLOGY

zebrafish embryos were collected and raised according to established procedures (Westerfield, 1993) and kept on a 12 hr 'on-off' light cycle, with light-on synchronized to embryo collection.

Animals of 3-11 days post fertilization were anaesthetized with saline containing 0.02% MS222 (Sigma), secured by insect pins to a Sylgard-coated dish, and incubated in HEPES-buffered saline containing (in mM): 100 NaCl, 2 KCl, 5 HEPES, 2 CaCl2, 1 MgCl2, (pH 7.3). For recording, one eye and the skin above the optic tectum was removed with forceps so that the tectal neurons came to lie exposed. 100 µM of the paralytic D-Tubocurarin was added to the bath to avoid muscle twitching. As shown previously (Zhang et al., 1998), this toxin treatment did not significantly affect the retinotectal responses. Finally, the animal was positioned on its side such that the remaining eye was facing directly down. Figure 6 displays the preparation how it was used for recordings and shows the neuropil cells that were targeted for visually guided patch clamp recordings.
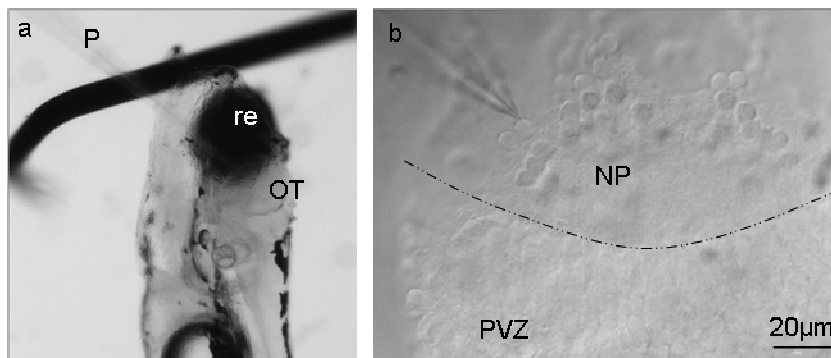
Figure 6: Preparation of zebrafish larva for patch clamp recordings
a: the larva is oriented on its side with only the right eye (re) remaining, the eye is facing down. From the top left corner the pipette (P) is visible; it terminates in the optic tectum (OT). b: high magnification of cells in the optic tectum. A pipette is patched onto a cell in the neuropil (NP). The dashed line marks the border to the periventricular zone (PVZ) where cell bodies lie densely packed.

For patch clamp recordings, silicate glass pipettes with a resistance of 10-15 MΩ were tip-filled with internal solution containing (in mM): 110 K-gluconate, 10 KCl, 5 NaCl,1.5 MgCl2, 20 HEPES, 0,5 EGTA (pH 7.3) and back-filled with the same solution additionally containing 200 μM Amphoterocin B (Sigma). The method of perforated-patch whole-cell recording has been described previously (Hamill et al., 1981;Rae et al., 1991). Experiments were performed at room temperature (22 °C). Recorded signals were amplified with a patch-clamp amplifier (Axopatch 200b). The signals were filtered at 1 kHz, sampled at 5 kHz, and recorded with custom written software (National Instruments, Adam Kampff) on a standard PC. The recordings were made near the resting potential of each cell which was generally around -55mV and therefore below the reversal potential for Cl- current (E_i ~45mV), which was determined by the disappearance and the reversal of spontaneous GABA (γ-aminobutyric acid)-mediated synaptic currents as the holding potential was changed towards more depolarized values.

3.2 VISUAL STIMULATION

Cells in the neuropil were patched under visual guidance (Olympus 40x water objective) and tested for light sensitivity with a simple light flash of the microscope illumination.

The remaining eye was oriented downward facing a diffuser which functioned as a projection screen. A commercially available video projector (Mitsubishi) was used to project visual stimuli via a mirror onto the diffuser. An area of 100x100 degrees was illuminated below the fisheye; the rest of the projection light was blocked out with a pinhole. Visual stimulation and data acquisition software were linked such that the onset of data acquisition was triggered by the stimulation software. Both were custom written in the lab (Adam Kampff). A schematic arrangement of the set up is drawn in Figure 7.
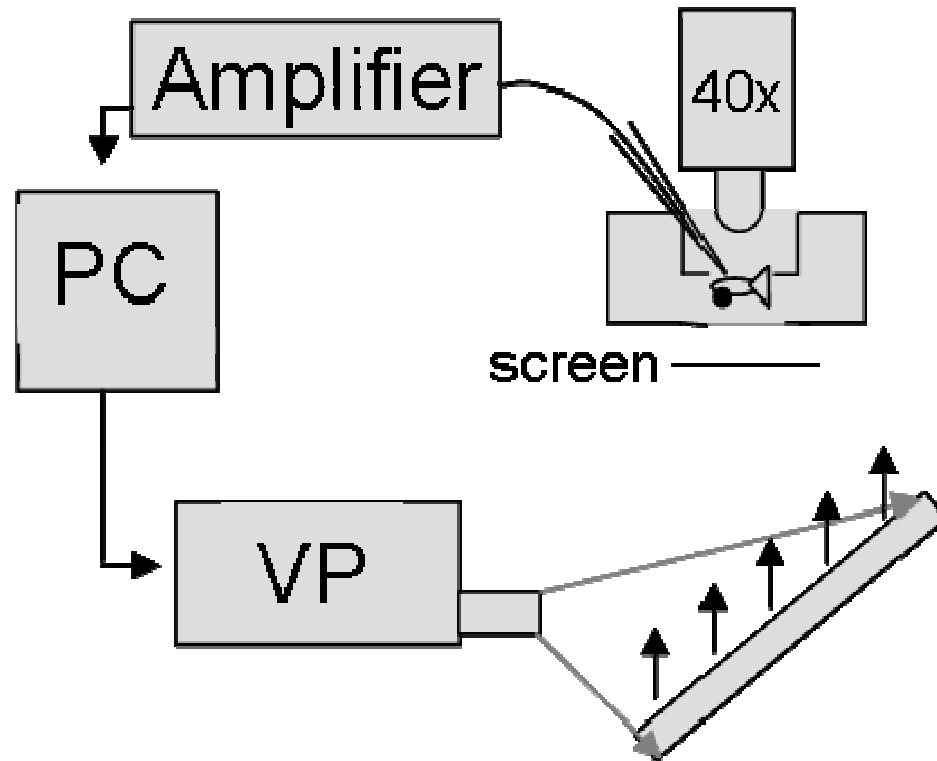
Figure 7: Set up for visual stimulation and *in vivo* patch clamp recordings
The larva is pinned into a Sylgard dish with the remaining eye facing down onto a 100x100 degree screen. A video projector (VP) is used to present images onto the screen, by reflecting them off a mirror (arrows). The computer with which the stimulus images are created is also used to record the electrophysiology data. Patch recordings are made under visual control (40x Objective) and amplified with an Axopatch 200b amplifier.

The following stimulus sequence was presented to all cells in this order (time permitting):

Light sensitivity

The cell's light responsiveness was measured for 30s with a whole field 'on-off' illumination at 0.5 Hz.

Natural movie

Given a reliable response to the light, 4 repetitions of a natural movie were shown for one minute each. For some cells different movies were presented. Sample frames of different movies are presented in Figure 8. Sparse and dense distributions of paramecia of different sizes are moving around in all 4 quadrants of the visual screen. The stimulus sequence was continued only if the responses to the movies were reliable across trials.

Temporal moments

To measure the whole field moments a sequence of 16 linear grey values (as measured from the brightness output of the projector) was flickered in a Gaussian pattern at 60Hz (monitor update rate) for 3 minutes. A schematic drawing is shown in Figure 9.

Static spatial receptive field

In order to measure the static receptive field the entire projection area was divided into a 4x4 grid. Dark squares (corresponding to each element of the grid) were flashed for 1s on a light background followed by a 1s (light) background illumination of the whole area in a pseudo random manner. A schematic drawing is shown in Figure 9. In several cases the receptive field was also measured at opposite contrast (white square on black background).

Dynamic spatial receptive field

To measure the spatial and temporal receptive field together, a filtered noise stimulus was presented at 60Hz for 5 minutes. The cut-off frequency was estimated with previously obtained knowledge about receptive field size. About 30% of the highest frequencies contained in a 100x100 white noise stimulus were cut out to obtain the filtered stimulus. The generation of this stimulus is shown in Figure 3. The consequences of choosing stimuli with a too small range of frequencies are shown in Figure 4.

Size and motion query

To determine whether the responses are linear to stimuli of different sizes, motion, and direction, a series of dots was either flashed inside the RF (10 sizes) or moved in 4 directions through the RF (8 sizes). The spots were used in the preferred contrast and were flashed at 1Hz or moved at 100deg/sec, respectively. Several repetitions of a whole series (size query stimulus) were presented.

End of stimulus period

Finally, time permitting, more repetitions of the initial natural movie were presented, or the cell was tested with different movies.
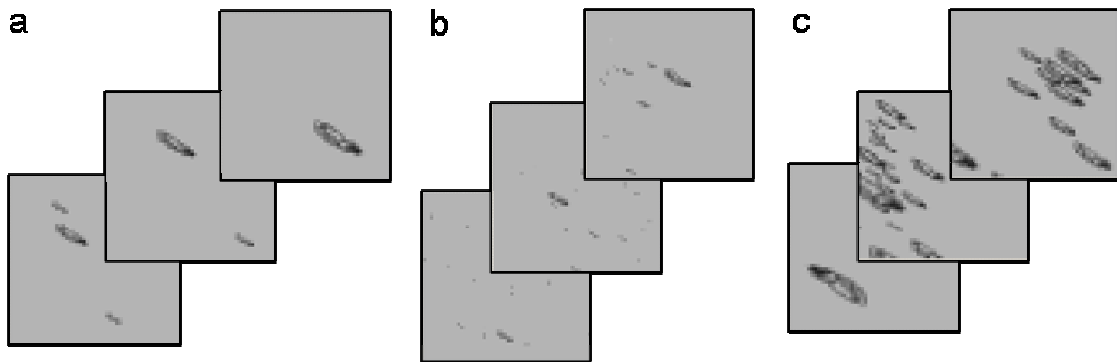
Figure 8: Example frames from 3 different simulated natural movies
3 types of paramecia simulations were shown, in which the density and size of paramecia was different. In all movies the paramecia were moving through the whole visual area.
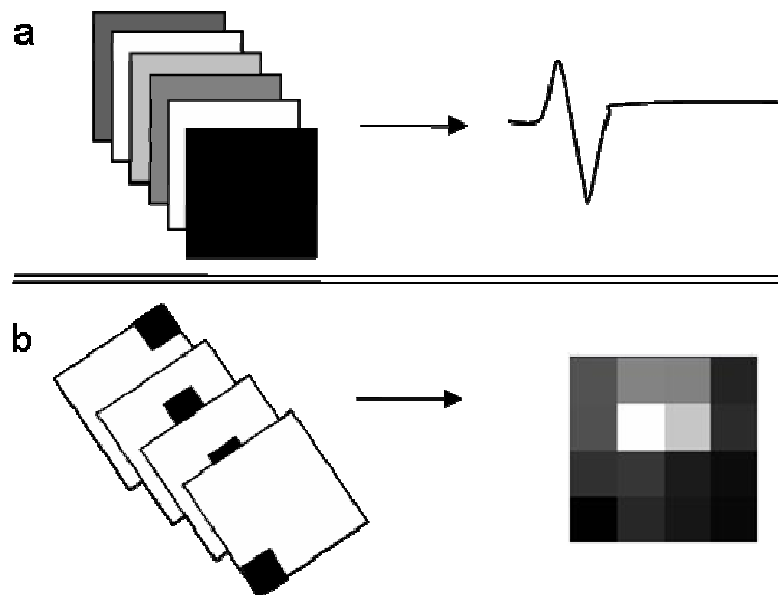
Figure 9: Schematic presentation of stimuli used to measure the temporal moment and the spatial receptive field separately
a: a sequence of 16 linear grey values was flickered at 60HZ for 3 minutes to calculate the temporal moment (cross correlation of stimulus waveform and recorded responses). Duration of the shown moment is 1s. b: to measure the spatial receptive field a pseudo random sequence (every square equally often in different order) of single squares was presented. Each square is 25 degrees and is flashed for 1 second. The squares are dark and flashed on a light background because the generated 'off' response was usually more prominent than an 'on' response. Sample traces can be found in Figure 15.

27

3.3   DATA ANALYSIS

Electrophysiology data for static measurements (light flash and receptive field) was binned down 5 times to reduce computational efforts. Data for dynamic measurements (moments and movies) was binned to the frame rate of the stimulus (16.7ms). In some cases the data was additionally binned down by a factor of 10 (noted where applicable).

Temporal moments

The temporal receptive field (moment) was obtained with reverse correlation. The electrophysiology recording was convolved with the linear Gaussian white noise stimulus sequence (Dayan and Abbott, 2001), (Marmarelis, 2004). To determine whether a moment is monophasic or biphasic, the moment amplitude was normalized to 1 for 'on' moments and -1 for 'off' moments respectively after baseline correction. The length of the moment was chosen manually, typically so that the end of the moment was set to the time point when it finally returned to baseline. The mean of the moment was calculated. A small mean signifies a biphasic moment, that has a positive and a negative component which cancel each other out, whereas a higher mean is the result of a monophasic moment, 'on' or 'off', respectively. Cells were grouped according to the age (in days) of the fish they were recorded from. The mean "mean moment value" was plotted for each group and values of one age group were compared to cells in other groups with the help of the student's T-test (Microsoft Excel). Furthermore a threshold value was determined by visual inspection, below which all cells with that value showed a biphasic moment. Cells of different ages were grouped (for example under 7 days vs. above 7 days) and then compared with respect to what percentage of cells was below this threshold (= biphasic) for each "young" and "old" group. Furthermore it was determined whether a moment was 'on' or 'off' by noting the sign of its mean, that is a positive mean was accepted as an 'on' moment whereas a negative mean was counted as an 'off' moment. Biphasic moment therefore fell into the category of their larger deflection.

Static spatial receptive field

The spatial receptive field was assayed by measuring the integrated charge of the 'off' and 'on' response of CSCs within a defined window (~200ms) for each stimulation square. The

spatial extend of the RF is displayed in three different ways. In the raw form, every square of the grid is assigned a grey value according to the normalized response size it evoked. Second, an interpolation algorithm, where each square is weighed with respect to its neighboring squares, is used to smooth the borders of the receptive field and third, a threshold is set to obtain a binary receptive field. The threshold was first determined by eye for every cell individually, and then the mean threshold for all cells was used to determine receptive field size for all cells that is comparable between different cells. The receptive field is marked in white in all cases, independent whether the response were 'on' or 'off'.

Dynamic spatial receptive field

Receptive fields measured with spatially filtered noise were calculated by 2 dimensional reverse correlation. The stimulus bmp (Figure 3) at each time frame was cross correlated with the current sweep and averaged. This yields the area of the whole stimulation window that consistently evoked a (large) response. The temporal moment is calculated from the receptive field area by cross correlating the light intensity fluctuations within that area with the evoked currents. The color code is adjusted such that black areas define 'off' responses and white areas 'on' responses. To determine whether the frequency spectrum of the stimulus was sufficient to describe a receptive field without under-sampling, the FFT of both, the receptive field and stimulus was taken and compared in their respective extensions (Figure 4).

Size and motion query and natural movies

For the size query experiments, several repetitions are aligned and responses to the same kind of stimulus are regrouped in order to be displayed together (see Figure 21). The integrated charge within a time window (~500ms-1s) was used to calculate the relative response amplitudes for a given size or direction/motion.

For experiments using the size query and natural movies, CSCs were aligned and cross correlated to obtain estimates of their trial to trial variability. The correlation index was calculated by dividing the mean of the cross correlations by the mean of all autocorrelations. Very similar sweeps will yield a correlation coefficient close to 1 and different sweeps will have a value close to 0.

Calculation of predicted responses

To calculate the responses to natural movies, the stimulus bmp at each time frame was multiplied with the spatial receptive field and each movie-pixel was convolved with the temporal moment. Furthermore an instant non-linearity was added to account for the fact that the CSCs at the chosen holding potential (around -55mV) are usually only inwards (negative) and that the response amplitude saturates at a certain level. This nonlinearity was obtained from the whole field white noise stimulation by plotting the data point by point over the prediction value. A second order polynomial function was fitted to this data cloud and the resulting function was used as the non-linearity in the model.

Two different spatial receptive field models were assumed and tested for each cell. In the first case, one response event was assumed to happen whenever the light intensity changed anywhere within the receptive field. The disadvantage of this "cylinder shaped" receptive field model is that objects entering the receptive field will only result in one response, when the object enters the receptive field (and depending of the contrast preference of a given cell, again when it exits the RF). While the object is within the receptive field, this model will not account for objects that move around within the receptive field. If cells are sensitive to the motion of objects, the responses size could be under-predicted this way. The second approach therefore included a substructure of the receptive field. The whole receptive field was divided into several sub-fields (each pixel within the RF area) that predicted a response increase whenever the light intensity changes in one of them. This addition accounts to some extend for increasing the response size for objects that have entered the RF and keep moving around in it. For every cell, the spatial receptive field model that yielded the best r^2-direct value (see next section) was applied.

Goodness of fit

The quantification of how well the predicted responses fit the measured data can be done by evaluating the r^2-value (r^2) in two different ways: this value is calculated by plotting the data versus the prediction and taking the linear regression (calculating how far the individual points are away from a line that is fitted through all points). Another way to quantify the prediction fit is to calculate the r^2 directly (r^2-direct). This is done with Equation 1. For a good prediction, the difference between prediction and data is smaller than the difference between a horizontal line through the mean and the data. This will

result in a d^2-direct value close to 1 when the prediction fits the data well and close to 0 if the prediction fails to fit the data any better than the horizontal line through the mean.

$$1 - \frac{\dfrac{\sum(PR-Data)^2}{n}}{\dfrac{\sum(Mean-Data)^2}{n}}$$

Equation 1: Quality of fit
PR is the prediction value at each time point, Data is the data value at each corresponding time point. Mean is the mean of all data values. A successful prediction fits the data better than a horizontal line through the mean. For a good prediction a value close to 1 will be obtained, whereas a worse prediction will result in a value close to 0.

3.4   STIMULUS PROTOCOL SUMMARY:

The entire stimulus protocol is summarized below for convenient reference:

- 1) Whole field light flash (30s, 0.5 Hz)
- 2) 4 repetitions of a natural movie (1 minute each)
- 3) Linear Gaussian White Noise whole field flickering (3-5 min, 60Hz)
- 4) Spatial receptive field measurement of 1 or 2 different contrasts (3 min, 1 Hz)
- 5) Several repetitions of moving and stationary dots of different sizes (2 min each)
- 6) More repetitions of a natural movie sequence until the cell died

Cells that did not survive through the entire stimulus sequence could partly be used for analysis of the data that could be collected.

4   RESULTS

In spite of the zebrafish's increasing popularity as a model system in visual research, little is known about the functional properties of the central visual system in adult and larval zebrafish. More than 20 years ago a study by Levinthal and colleagues described receptive field properties of cells in the periventricular zone with extracellular recordings in adult fish (Sajovic and Levinthal, 1982a;Sajovic and Levinthal, 1982b;Sajovic and Levinthal, 1983). Only recently has one functional study followed up on these results and described similar properties in larvae with the use of calcium imaging (Niell and Smith, 2005).

The work presented here is the first that describes the characteristics of cells in the neuropil of the optic tectum in larvae. It is also the first patch clamp study in this system, a method that provides insight of sub-threshold signals with high temporal resolution in the tectal cells.

4.1   RESPONSES TO VISUAL STIMULI

Synaptic currents were recorded from cells in the tectal neuropil of larval zebrafish using in vivo perforated patch clamp techniques. Typically, the cells were held at a holding potential of -55 to -70mV to be close to their measured resting potential. A custom build visual stimulation set up together with custom written stimulation software was used to present several different visual stimuli to the immobilized fish. A standard stimulus protocol was presented to 12 cells. The protocol was determined by measuring neuronal responses to numerous different visual stimuli in several hundred neurons beforehand.

By observing the system in this exhaustive way a general impression could be obtained of what type of stimuli the cells respond well to. Some of the preliminary test data could also be used in the final analysis. A full description of the resulting test protocol can be found in the methods section. Briefly, the cells were tested for response invariability to a natural-like movie. Cells that did not respond reliably to the movie were not included. If the cell did respond reliably to 3 or more repetitions, the spatial RF was measured by flashing 25 deg squares across the visual field (4X4) at 0.5Hz. The temporal kernel was

measured with a whole field Gaussian white noise flickering at 60Hz. An additional measurement of the neuron's preference/ selectivity for size, motion, direction/orientation, and its contrast in-/variability followed. This was done by flashing or moving different size dots in 2 different contrasts in the RF. Preliminary experiments using two dimensional filtered noise stimuli revealed that these neurons are space time separable. The separation of the different kinds of stimuli is therefore applicable.

Surprisingly, none of the measured cells showed strong direction selectivity in contrast to what has been reported for PVZ cells in the tectum of zebrafish and tadpoles (Niell and Smith, 2005). However, in some cases there was a preference for one orientation of motion when tested with a moving dot in 4 directions. Virtually all cells responded better to moving stimuli than to stationary stimuli of comparable size; in some cases responses were bigger for small stimuli than to big stimuli, both moving and stationary. The responses to different stimuli are described in detail in the following chapters.

All cells included in this study responded readily and with little variability to a natural movie. Several different natural movies were used. Different cells are presented below.

4.1.1   RESPONSES TO WHOLE FIELD LIGHT FLASHES

All visual stimuli were shown on a 100x100 degree screen. To test for the cell's light sensitivity the whole visual field was illuminated for two seconds followed by a two second dark period (stimulus onset and duration are indicated by the grey bars above the responses in Figure 10). Several different response qualities could be identified which indicate the involvement of diverse (retinal and/or intertectal) input channels converging onto tectal cells. Different response kinetics were detected that point toward a combination of a variety of ion channels that compose the currents (compound synaptic currents (CSCs)).The whole field responses for 6 different cells are shown in Figure 10.

As a general rule it can be stated that virtually all cells have a response to the light going 'off' while cells with pure 'on' responses could not be found with this method (but see temporal moment data). One can distinguish between two general groups of cells: cells that respond with similar current amplitude to both, 'on' and 'off' stimulus ('on/ off' cells, Figure 10a) and cells that have a preference for either stimulus ('on'- or 'off' cells Figure 10b and

c). Furthermore one can make the distinction between cells that are only transiently active during contrast changes (Figure 10a-c left panel) and cells that are continuously active throughout the time the light is 'on' or 'off', respectively (Figure 10a-c right panel). 60 cells were included in this analysis for the whole field stimulus. Among all the analyzed cells all possible combinations of these characteristics ('on' or 'off', -transient or -continuous) could be found. 6 sample cells are displayed in Figure 10.
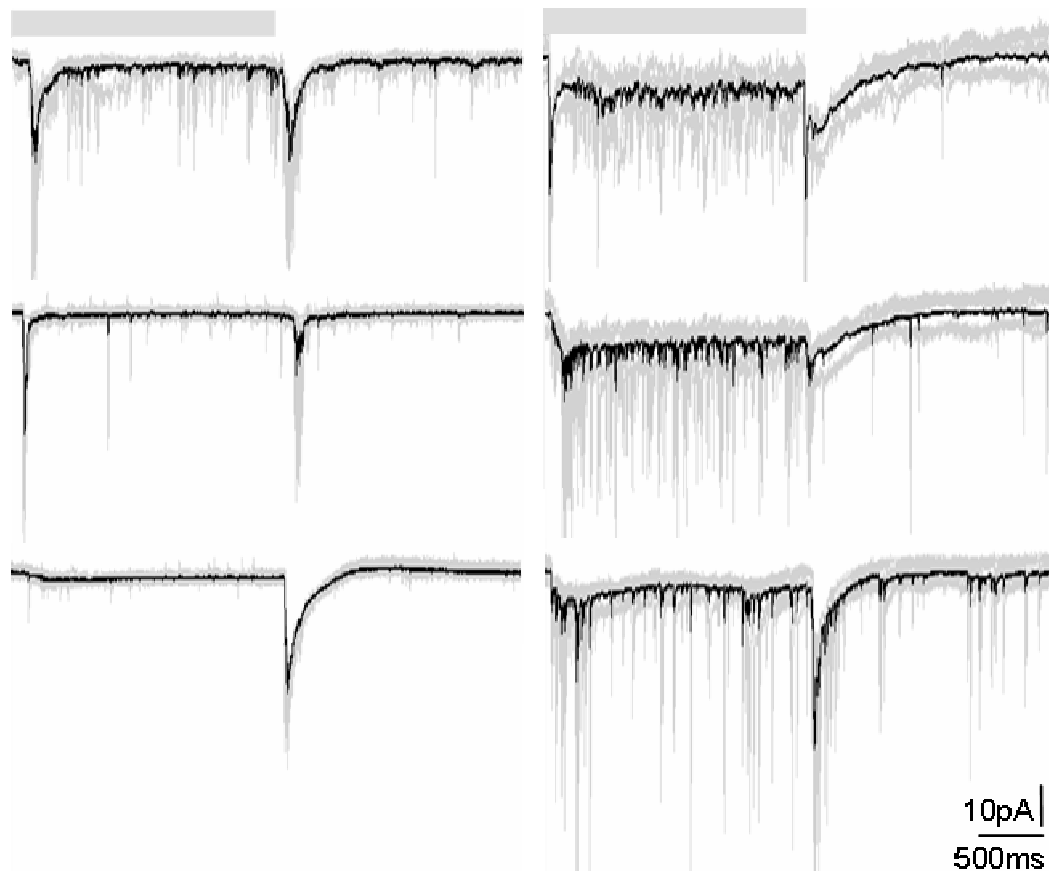

Figure 10: Responses to whole field changes in light intensity
Average responses of 6 different cells are shown in black, the 7stimulus repetitions raw data are shown in grey. A whole field light change was shown at 0.5 HZ, the duration of light 'on' is indicated by the grey bar above the top panel and is valid for all panels. Top: both cells respond equally well to light 'on' and 'off', middle and bottom: either the 'on' (middle) or the 'off' response (bottom) dominates. Left side: cells only respond transiently to changes in the light intensity. Right side: additionally to the transient responses, a tonic response can be seen for the whole stimulus duration. Different response kinetics could be observed that include fast and slow responses and a combination of both. An example for a fast responses can be seen in the 'on' response of the middle left panel (~50ms), a much slower response in the 'off' component of the bottom left panel (~500ms plus after-hyperpolarization) and the combination of fast and slow component is seen in the 'off' response in the top right panel.

4.1.2   TEMPORAL RECEPTIVE FIELD PROPERTIES

Temporal receptive fields or moments are measured by cross correlating the stimulus waveform (a whole field flickering Gaussian white noise) with synaptic currents that were elicited by this stimulus. Examples of temporal kernels (moments) are shown in Figure 11.

Several different types of temporal kernels can be observed, most prominently one can distinguish between 'on' and 'off' moments that can be either mono- or biphasic (Figure 11a and b respectively). Very few cells have a pure 'on' moment (right panel, Figure 11a). The large majority of cells respond best to a light going 'off' as depicted by a down deflection of the moment in Figure 11a (left). This strong preference for 'off' responses has also been observed for cells in the optic tectum 'off' Xenopus tadpoles and adult zebrafish (Engert et al., 2002;Vislay-Melzer, 2005)
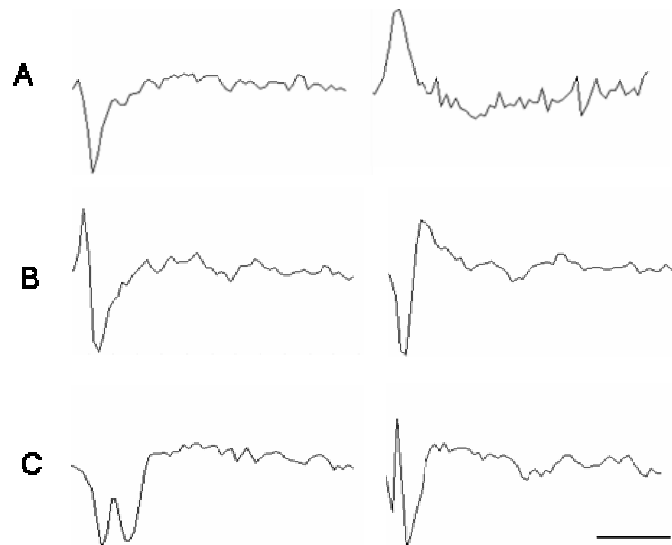

Figure 11: Different temporal kernels (moments) of 6 representative cells measured with a whole field flickering light stimulus at 60Hz.
Light decreases are shown as downward deflections of the moment. Time is given on the x-axis, scale bar=250ms. The y-axis is given in normalized arbitrary units. Time 0 on the left indicates the beginning of the convolution filter. a: monophasic 'off' (left) and 'on' (right) moment. Delay and duration of each moment varies from cell to cell. b: 2 biphasic moments where the 'off' moment is either preceded (left) or followed (right) by the 'on' component. c: temporally overlapping 'off' and 'on' moments result in a triphasic kernel where an 'on' peak lies within the downward deflection of the moment. It indicates that the cells respond equally well to light independently going 'on' or 'off' and has two preferred stimuli with a slightly offset delay and different amplitudes.

The preferred 'off' moment is often preceded or followed by an 'on' moment which results in the biphasic moments shown in Figure 11b. In biphasic moments one can distinguish between moments where the first component is stronger or weaker in amplitude than the second component independent of the sign of deflection. These two types of moments have previously been described for cells in the mammalian LGN. There, one can find non-lagged and lagged cells with moments where the first or second deflection dominates, respectively (Saul and Humphrey, 1990).

Figure 11c shows kernels of 2 different cells where the 'on' and 'off' component are overlapping temporally but they can still be separated with reverse correlation techniques because of a temporal offset. This results in a triphasic moment. It indicates that the cells respond almost equally well to light independently going 'on' or 'off' (contrast invariant cells) and have two preferred stimuli with a slightly offset delay and different amplitudes. The 'on' peak in the middle of the 'off' deflection is only detectable with the reverse correlation because of the different delays and kinetics. For equal 'on' and 'off' timings and amplitudes one cannot obtain a moment with reverse correlation because both, the 'on' and the 'off' contributions, cancel each other out, resulting in a more or less flat line. If one moment component dominates strongly in amplitude over the other, it would "win" and result in a monophasic moment given that the temporal dynamics were largely identical between 'on' and 'off' components. Such triphasic temporal moment fluctuations have previously been described for approximately space-time separable receptive fields of simple cells (DeAngelis et al., 1993a;McLean et al., 1994).

In mammalian LGN cells maturation of temporal characteristics usually takes longer to occur than maturation of spatial receptive field properties. It has been shown that biphasic moments are less likely to be found in younger cells, whereas in older cells the majority has biphasic moments (Cai et al., 1997). In the age range studied in larval fish in the present work, a change was observed with respect to the biphasicness of moments when comparing young and old group (without the 11 dpf group).

Figure 12 summarizes the analysis for the temporal moments across different age with respect to the biphasicness. In the top panel the mean biphasicness is plotted for each age group together with the SEM. Mean biphasicness was determined for an individual length for each moment (see Figure 13). The x-axis displays the age of each group in days post

37

fertilization. A trend line was fitted to all age groups (black line) that displays a small decrease in values (=more biphasic) for older fish. However, this trend might only arise from the 3 day group which is an outlier in the distribution and furthermore only consist of 2 cells. The grey line was fitted to the data omitting the 3 day group and no decrease can be observed.

The middle panel shows the percentage of cells that were considered biphasic for different age groups. For this analysis a 'biphasicness-threshold' was set. Below this threshold a cell was considered biphasic. The threshold was determined by visual inspection of many moments and was set to 0.15 au. Cells were grouped into either belonging to older (dark grey) or younger (light grey) with a varying threshold as shown on the x-axis. The y-axis displays the percentage of biphasic cells. A line fitted through the younger group data (light grey bars) indicates a small increase in percentage of biphasic cells with increasing age. Interestingly, the oldest group (dark, <11) shows the smallest percentage of biphasic cells. For younger cells the percentage of biphasic cells was consistently lower than for older cells. A student t-test comparing young and old yielded little significance (p-value= 0.09) but when the oldest group (11d) was omitted the difference in percentage of biphasic cells between young and old was highly significant (p=0.0001).

The lowest panel depicts the ratio for monophasic/biphasic cells for the same groups as in the middle. The respective older group is shown in dark grey, the younger group in light grey. A decrease in the ratio of mono-/biphasic moments could not be observed.
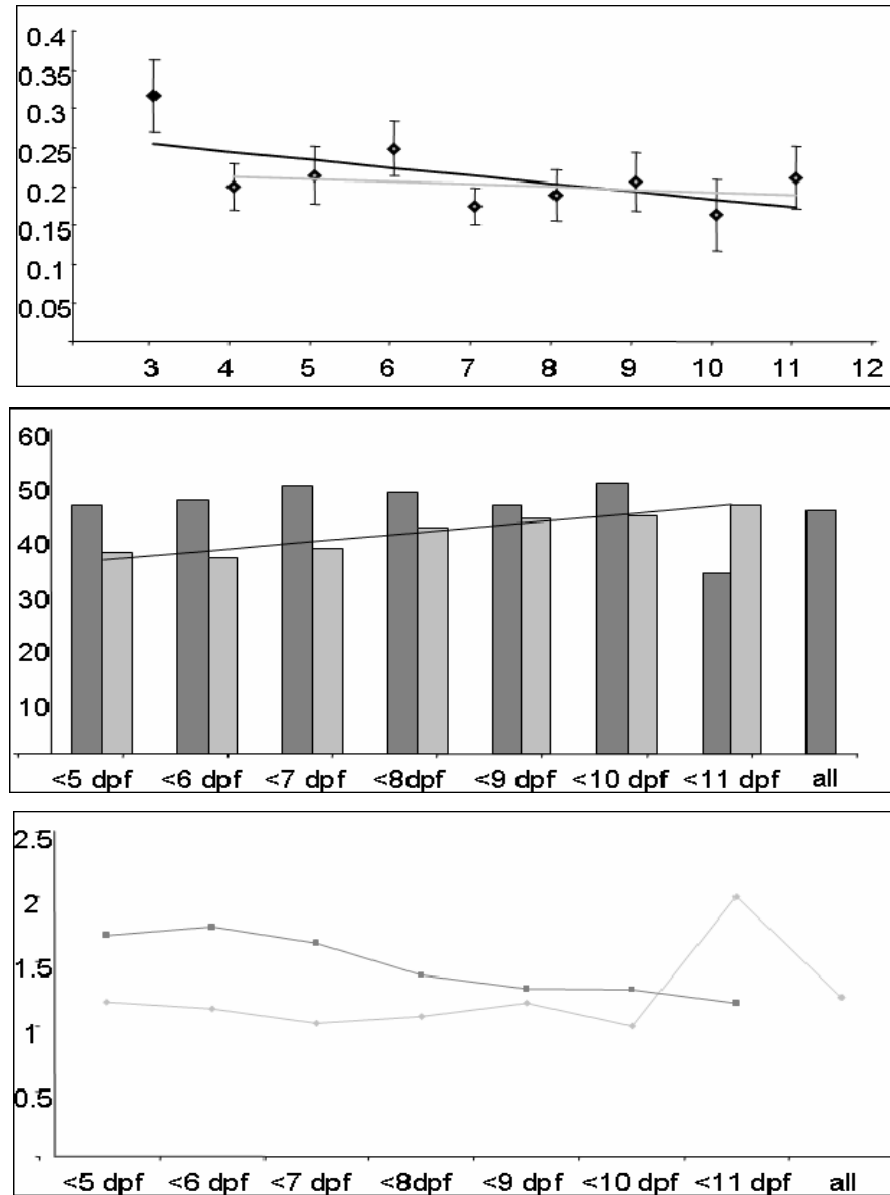
Figure 12: Biphasicness of moments for all age groups
Three different analysis methods for the biphasicness of their moments are shown. **Top**: mean biphasicness of the moments (Y-axis) is plotted with he standard error of the mean (SEM) for fish of each age group (black). Age is given in days on the x-axis. The grey line is fitted to all ages except 3days to display that the eventual trend of a lower values for older fish might be due to an outlier which consists of the 3 day group (n=2, see text). **Middle**: A maximal value of 0.15 was determined visually for moments to be regarded as biphasic. This threshold was used to determine what percentage of cells lies above and below this threshold at different ages. The X-axis displays the age group of the fish in days post fertilization (dpf), the Y-axis the percentage of cells that were under the threshold at a given age (% of biphasic cells). Dark grey displays older cells, light grey younger cells. The fitted line indicates a trend towards more biphasicness the more older cells are added to that group. **Bottom**: ratio of monophasic cells to biphasic cells as determined with the threshold used in the middle panel for older cells (dark) and younger cells (light grey). N=150cells.

Figure 13 displays the analysis of the total length of the moments arranged into age groups. A fitted line suggests a minor trend for moments to become slightly shorter in their overall duration; however, this effect was not significant. Furthermore the slope of the trend line results from the 3 day outlier, a group that consists only of 2 cells and must therefore not be over-evaluated. All in all it can be concluded that no obvious temporal refinement takes place during the whole observed time period but a significant change occurs with respect to the percentage of biphasic cells between day 3 and 10.
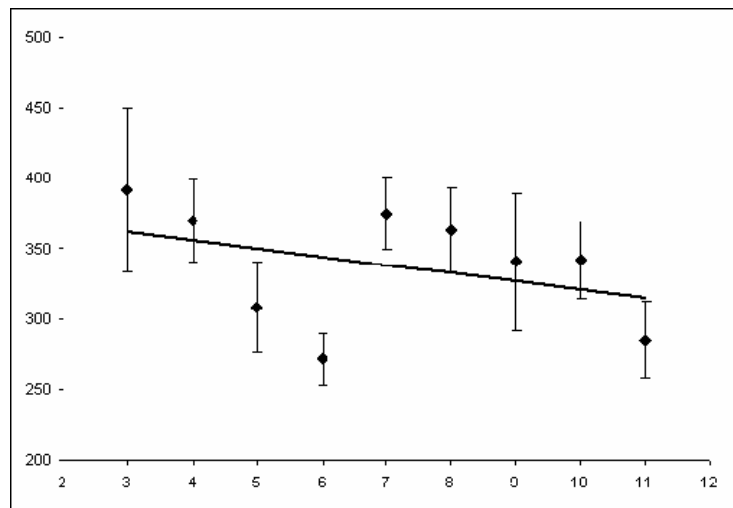

Figure 13: Total length of moments for all age groups
The total length of moments was analyzed for 150 cells and grouped according to the age of the fish. The average moment length at each age is shown with the standard error of the mean for fish 3-11dpf. The X-axis marks the length as determined by visual inspection.

The qualities of the moments undergo changes with increasing age, that is the percentage of 'on' and 'off' cells varies over age. Figure 14 shows that the youngest cell group (3-4dpf) has more 'off' moments whereas in the oldest group (10-11dpf) has more cells with 'on' moments (top panel). A moment was grouped either category by sorting whether the mean of the moment was positive ('on' moment) or negative ('off' moment). Biphasic moments were grouped with their dominant part. The bottom panel shows that the switch between 'off' cells to 'on' cells being the prevalent group occurs between day 8 and 9 where both kinds of moments are almost equally often present.

40
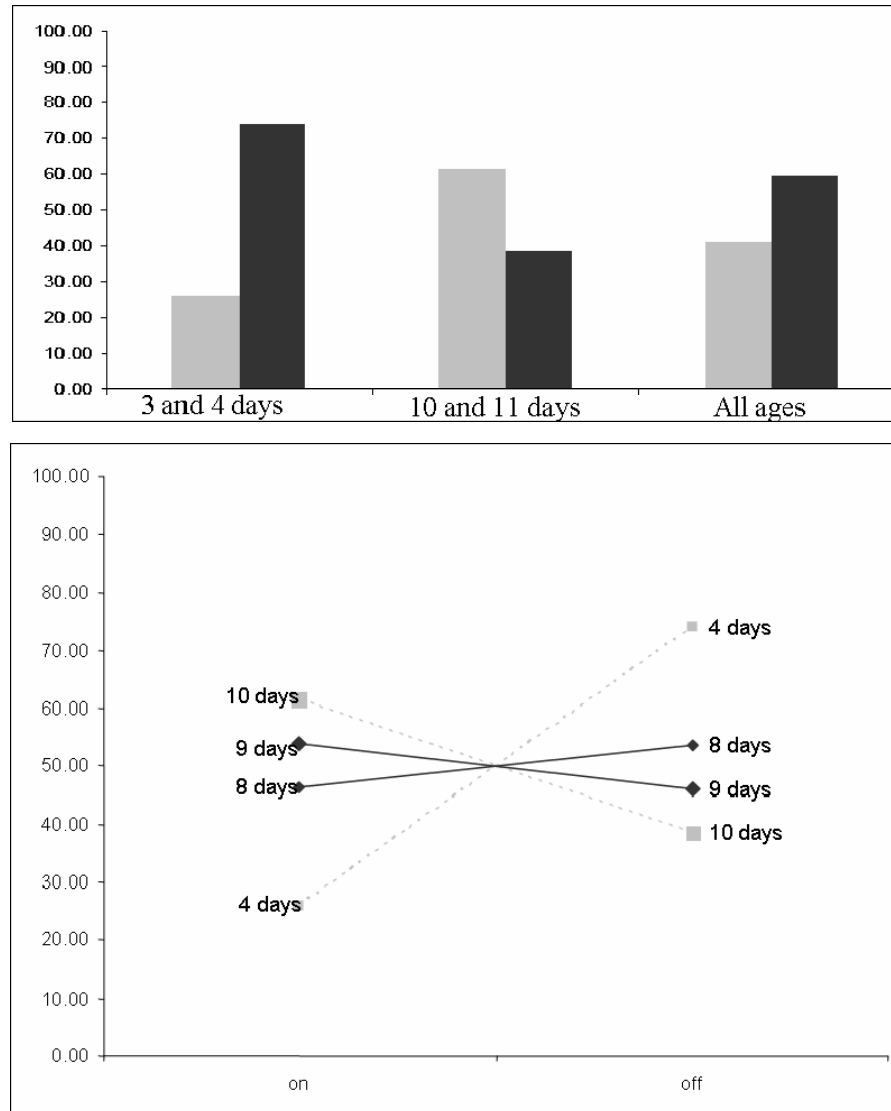
Figure 14: Distribution of 'on' and 'off' moments over age
Top panel: Light grey bars represent the percentage of cells with an 'on' moment, dark grey bars represent the percentage of cells with 'off' moments. Biphasic moments were grouped in their dominant category. 74% of cells in the younger group have an 'off' moment, whereas in the older group has only 38% 'off' cells. For all ages together a 60/40% distribution occurs for 'off' and 'on' cells respectively. Y-axis % of cells, X-axis age groups. Bottom panel: the switch between more 'off' cells to more 'on' cells occurs between 8 and 9 days. Y-axis: % of cell, X-axis 'on' and 'off' moment.

4.1.3 STATIC RECEPTIVE FIELDS

A typical receptive field for one cell is shown in Figure 15. Raw data, interpolated data, and threshholded data are displayed (Figure 15a and c, left to right). Typically these neurons show a compound response (fast and slow component shown in b and d) to a light

41

flash going 'on' and 'off' in a specific region of the visual field. Note, that in the display in Figure 15 the 'off' response is first, occurring around 100ms followed by the 'on' response at around 1100ms because of negative contrast of the mapping square relative to the background brightness (dark mapping spot on light background). The mapping was shown for one second in each position indicated by the grey bar. The current traces in b and d are taken from two different positions (marked by stars). In b, an 'off' ' and an 'on' response is evoked by the square marked with a star. In d however, only an 'off' response can be recorded. Since no 'on' response was elicited there, the overall area of the 'on' receptive field is smaller than the 'off' area.
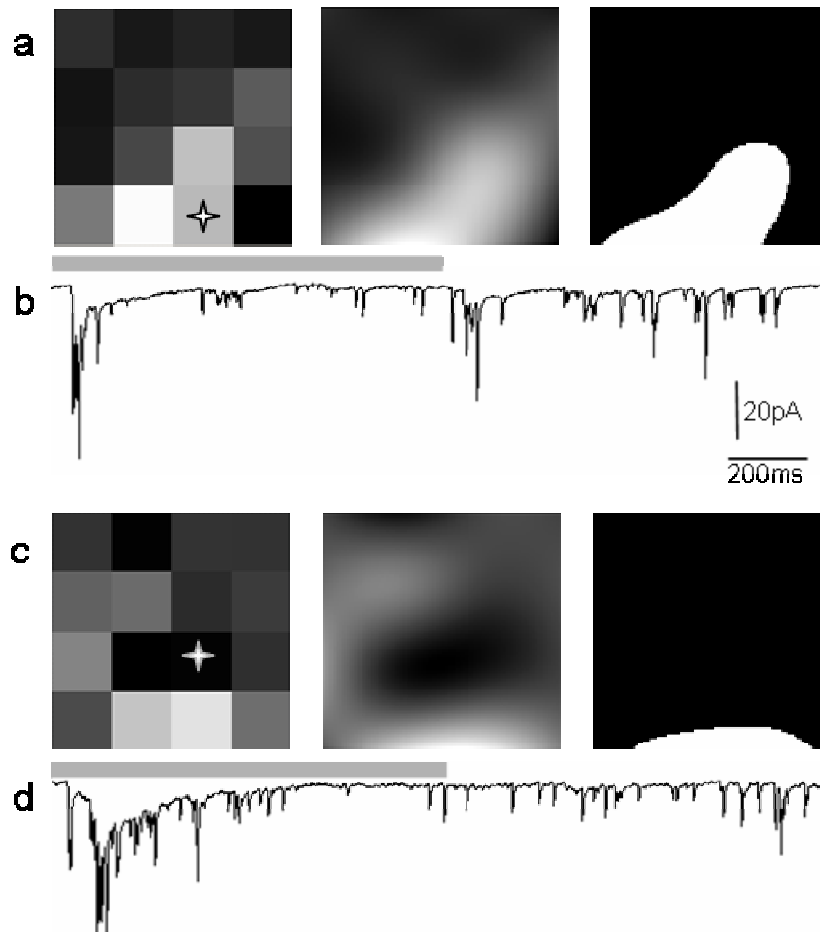
Figure 15: Representative example of a receptive field measured with a 4X4 grid in a 4 day old fish
A dark square (25 deg) was presented for one second (grey bar), followed by a one second background illumination (=on period). In a and c, 3 different displays of the same receptive field are shown for the 'off' response (a) and the 'on' response (c), respectively. Left: raw data where a grey value is attributed to every square according to the integrated charge it evoked, middle: grey values are normalized (0-255) and interpolated taking into account the value of each neighboring square, right: threshholded receptive field. The 'on' receptive field area is smaller than the 'off' RF field (8 degrees on, 17 degrees 'off'). In b and d average current traces of 5 trials are shown that display the responses to 2 different squares (marked by stars). b: an 'off' and an 'on' response is evoked by the square with the star in a. d shows the response to the square above that (marked with star in c), which only evoked an 'off' response resulting in a smaller 'on' receptive field. Note that the first response (around 100ms) is the 'off' responses due to a dark mapping stimulus.

Receptive filed size was calculated for 67 cells using the threshold display. A suitable threshold was first determined by eye for every cell to determine the mean threshold that was then used to define receptive field sizes comparable across cells. Receptive field size was noted in pixels and converted into degrees. The sizes of receptive fields ranged from

~5 degree to almost the whole stimulation field (~80°) with a mean of 17 degrees (+/-10) for an 'off' stimulus and 14 (+/-10) for the 'on' stimulus. Determining the receptive field with an individual threshold yielded an average receptive field size of 15 degrees (+/-9) indicating that a general threshold is suitable to compare between cells. Most cells have a stronger 'off' RF, spatially mostly overlapping with a weaker 'on' RF. A smaller 'on' than 'off' receptive field was found for 27 out of 67 cells and 26 did not have an 'on' receptive field at all.

Though varying in size and location between cells, receptive fields don't undergo spatial refinement during the observed period between 4 and 10dpf. The average 'off' receptive field size for the youngest fish (4dpf) was 18° and for the oldest group (10dpf) 18.75°. The lack of spatial refinement in this period of postnatal development is consistent with another report of larval zebrafish tectum cell function (Niell and Smith, 2005). One of the smallest and largest observed receptive fields are shown in Figure 16 and Figure 17 for animals 4 and 5 days of age respectively.
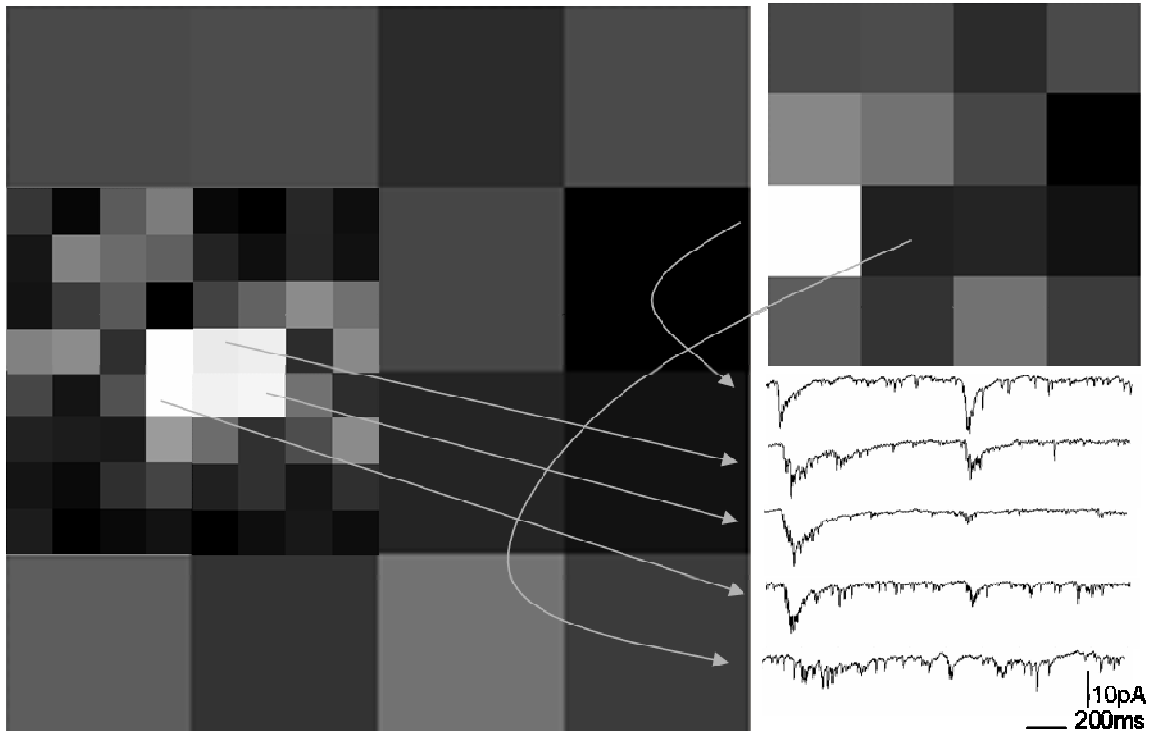
Figure 16: Small receptive field recorded from a 4 day old fish
Only the 'off' RF is shown. Top right displays the whole visual field with the white square representing the receptive field measured at low resolution. The high resolution inset left shows the sub structure of this receptive field. Average current traces from the contributing squares (marked with the respective arrows) are shown in the bottom right. Interestingly, only one high resolution square is responsible for the current evoked by the whole square. The evoked responses of small and large square stimulus are roughly the same in amplitude and length (sweep 1 and 4 on the right). Even though the responses to the other high resolution squares are also similar (sweep 2 and 3), those squares when presented as whole resulted in a much lower responses amplitude but with a longer duration (last sweep, black square next to RF in top right).
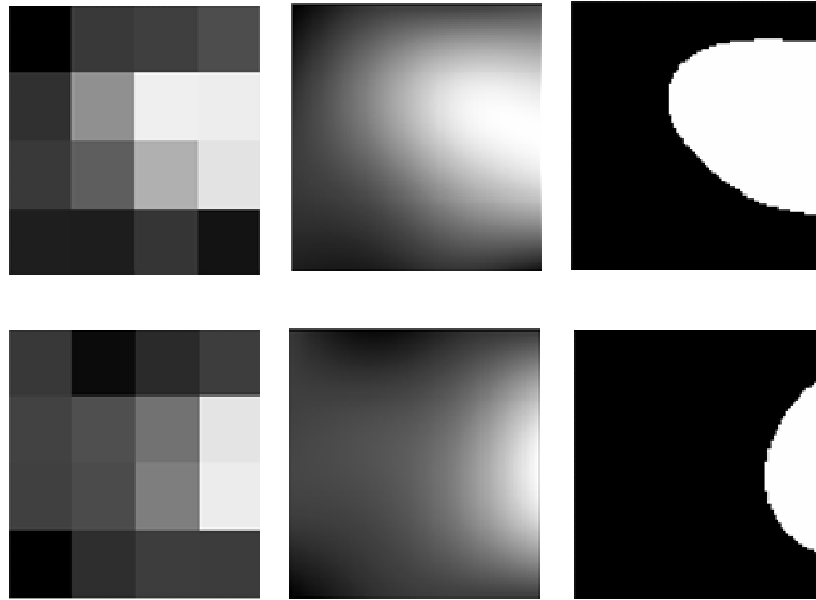
Figure 17: Large receptive field recorded from a 5 day old fish
One of the larger receptive fields is shown that spans over 40 degrees for the 'off' stimulus (top). The 'on' receptive field significantly smaller, it only comprises 2 squares resulting in 10 degrees (bottom).

Unlike cells in the PVZ, neurons in the neuropil do not show retinotopic organization of their RFs. The location of the RF of a neuron does not correspond to the neuron's location within the tectum. A potential explanation could be found in the morphology of these neurons. Large dendritic trees which can span up to half the rostro-caudal axis of the tectum (Naumann E.A. and Engert F., 2005) enable these neurons to possibly receive inputs from a large range of RGCs and therefore of many different locations of the retina coding for different locations within the visual field. Example cells, that don't have a retinotopic organization, are shown in Figure 18. Two caudal cells (top) and rostral cells (bottom) have receptive fields on opposite ends of the visual field. Furthermore, two cells that lie on opposite ends of the tectum (left pair and right pair) have receptive fields that code for the same area within the visual field. The retinotopic organization upheld in the periventricular zone would predict rostral and caudal cells to have a receptive field on opposite ends of the visual field.
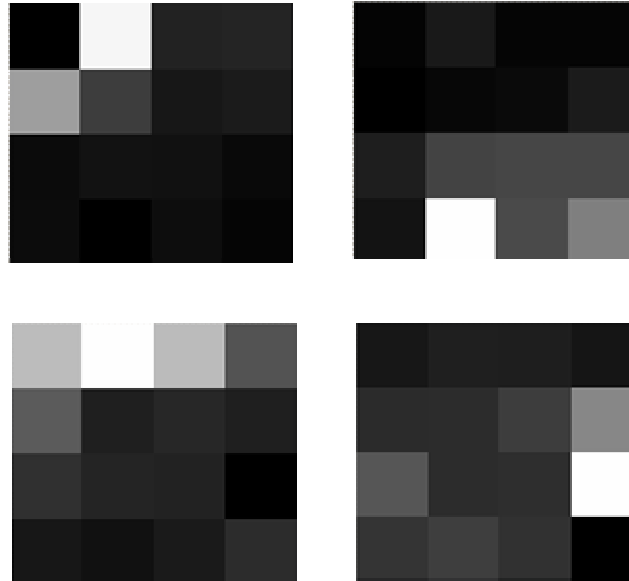
Figure 18: Neuropil cells don't have retinotopically organized receptive fields
Receptive fields of 4 different cells are show. The two top RFs were recorded from cells caudally in the tectum, the bottom cells lay rostrally in the tectum. Both caudal cells have receptive fields at different locations within the visual fields. Additionally, cells that have a receptive field in the same area don't need to lie next to each other in the brain (left top and bottom cell, and right top and bottom cell).

RF center surround-structured receptive fields could be expected from studies in other vertebrate brain areas that receive direct input from the retina like the LGN or superior colliculus in mammals. It seems however, that cells in the neuropil lack this type of center-surrounds structures. Neither with the static method, nor with two dimensional noise could center surround RFs be observed. In a specific attempt, where the cell was directly stimulated with concentric rings of different contrast, the response size wasn't altered when compared to the individual stimulation of either area (data not shown). An indication for an inhibiting surround could however been found with the stimulation of small and large spots (see size query section)

4.1.4   **RECEPTIVE FIELDS MEASURED WITH SPATIALLY FILTERED NOISE**

Two-dimensional white noise analysis has been successfully used to describe receptive field properties in many sensory systems (Marmarelis, 1991). As an unbiased method to measure characteristics of novel systems it has many theoretical advantages, however, a

critical experimental disadvantage is that the recordings need to be held up for a relatively long time. A way around this long recording time is to determine boundary conditions in separate experiments and use this knowledge to filter noise appropriately for a given system. For example one can determine the smallest spatial frequency that visual neurons can resolve and cut out all frequencies smaller than that. Schematically, this is shown in Figure 3. A series of experiments where the receptive fields were measured with spatially filtered noise and also with a slowly flashed mapping square are summarized below with one example cell to elucidate the differences and similarities of both methods for the temporal and spatial properties, respectively.

In Figure 19 the temporal properties of one cell are compared with two different measuring methods. The top panels were derived from stimulation with spatially filtered noise, the bottom panels were calculated from whole field stimulation with Gaussian white noise. In the first case, the temporal filter was calculated from the area inside the square. Both stimuli were shown at the update rate of the monitor (60Hz).

With both methods the temporal moment obtained is similar and depicts in both cases the main characteristics of a triphasic moment, starting with a fast 'off' followed by an 'on' component and ended with a slower second 'off' component. The exact timing of the second 'off' component is somewhat slower in the whole field experiment which might be due to the cells fatiguing during a second experiment and lies within trial to trial variation of repeated moment measurements. In general one can say that both methods reveal the same characteristics for the temporal measurement.
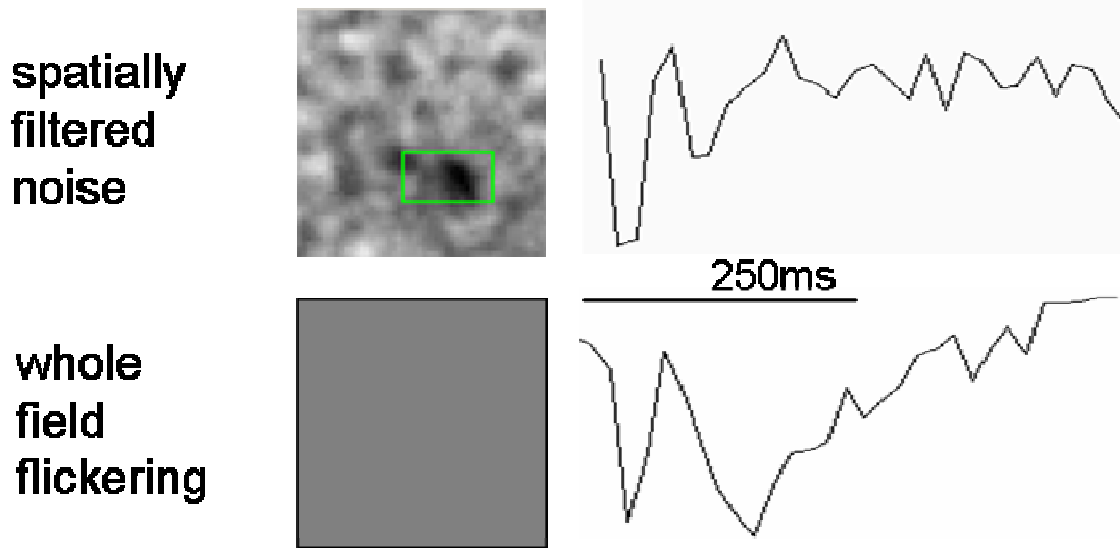
Figure 19: Temporal moment measured with spatially filtered noise and a whole field LGWN
The top panels show the spatio-temporal receptive field of one cell measured with filtered 2 dimensional noise. The dark area inside the square is the 'off' receptive field of that cell. The temporal moment for this cell (right panel) was computed from the area inside the square. The lower panels display the temporal moment measured separately from the spatial receptive field with a whole field Gaussian white noise flickering. Except for a slightly longer duration of the second 'off' part of the moment, both methods reveal a qualitatively similar result: a fast-'off-on' -slow-'off' moment.

The spatial receptive field measurements with filtered noise in comparison with the RF mapped with single dark squares are shown in Figure 20. Whereas in the latter case a receptive field is always shown as the white area, independent whether it belongs to the 'off' or 'on' component, the receptive field obtained with spatially filtered noise is color coded such that the 'off' receptive field is black and the 'on' component is white.

The top panels in Figure 20a display the characteristics of the receptive field calculated with the 'off' response and the bottom panels correspond to the 'on' response (top and bottom right). The first (left) panel shows the receptive field determined with filtered noise analysis. With both methods the location of the receptive field is the same, roughly the lower middle of the presented area. In contrast, the respective size of each receptive field measured with either method doesn't compare as well. In the case for the noise stimulation the receptive field area appears to be much smaller. Figure 20b shows a current sweep that was evoked by the flashing of the square marked with an Asterix. One can clearly distinguish an 'off' response in that area. This area however, is not part of the receptive field measured with 2 dimensional noise stimulus. This suggests that the

49

receptive field shown left is an underestimate of the actual area that the cell is responsive to.

A second difference between the two receptive fields is that in the first case where the receptive field was measured with noise, no 'on' component can be detected whereas the flashing method does evoke a response when the dark spot disappears (end of grey bar in Figure 20b) in 2 spots in the lowest row. However, the 'on' response is not as prominent as the 'off' response and also not present in the whole area of the 'off' receptive field but only in the lower part. The recording trace is an average of 5 repetitions of the square marked with an Asterix.
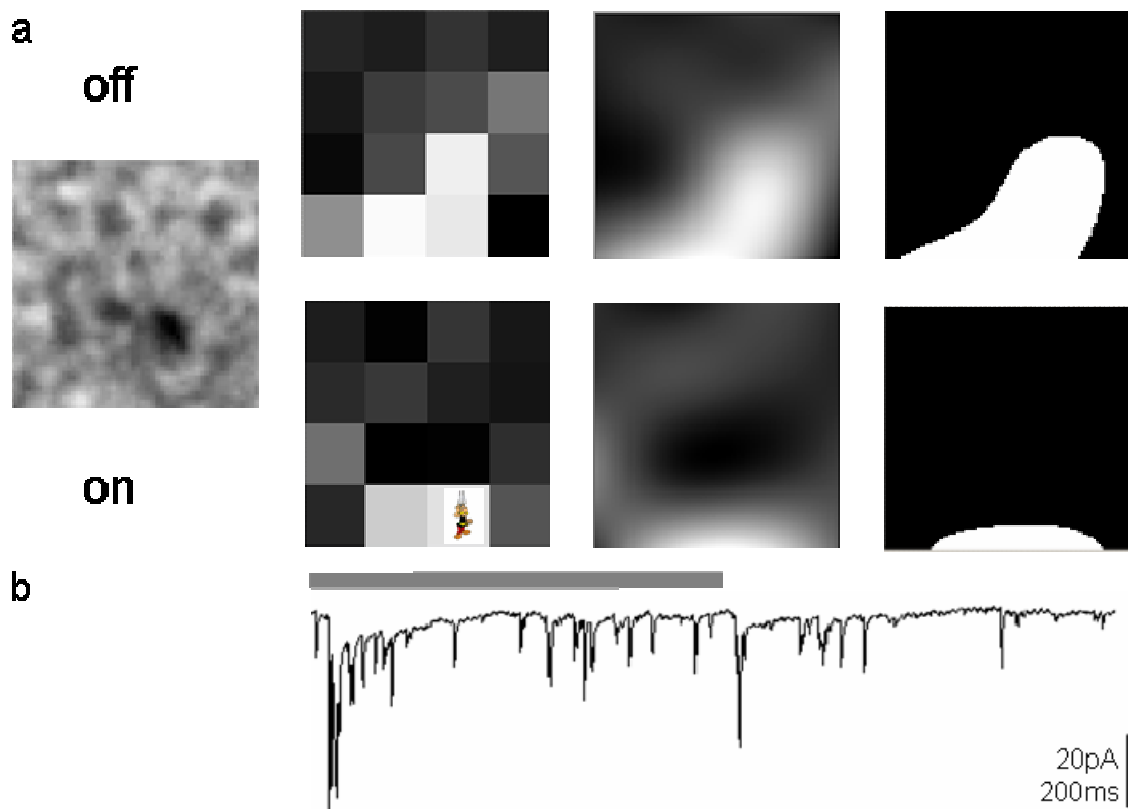
Figure 20: Spatial receptive field measured with filtered noise and a flashing square
a: The top and bottom panels on the right show the receptive field of the cell in Figure 19 in the raw, interpolated, and threshholded way for the 'off' and the 'on' component, respectively. The left panel depicts the receptive field as determined with spatially filtered noise. The display is chosen such that an 'off' response is marked with black areas and an 'on' response with white areas. Note that with the spatially filtered noise no 'on' component of the receptive field can be detected and that the receptive filed size is different for both methods. b: with the flashing spot, an 'on' response was elicited in 2 bottom row squares. The recording is an average of 5 presentations of the square marked with an Asterix.

The comparison between those two methods leads to the conclusion that both carry equal information about temporal properties and the rough location of a receptive field but yield different results with respect to detailed spatial characteristics. In this case both methods required about the same recording time. Taking the multiphasic moment of this cell into account it can be assumed that due to averaging techniques in the case of the noise analysis the weaker 'on' response doesn't get detected because of smaller amplitude and kinetics that lie within the 'off' response.

4.1.5 SIZE QUERY

The spatial and temporal receptive field characteristics determined up to this point can give conclusions about the "where and when" but do not allow for detailed understanding for "what" or even "how".

The following chapter focuses on experiments to determine whether cells in the neuropil are motion sensitive, direction selective, and linear in respect to their spatial summing mechanisms. To this end a stimulus composed of different sized dark dots on a white background was presented. Dots were both flashed and moved inside the beforehand determined receptive field area. For stationary dots, a series of 10 sizes was chosen from 5 to 60 degrees, each one was presented for one second. Moving dots of 8 sizes (omitting the 2 largest ones) were moved in 4 directions through the center of the RF. All the following tests were done with round dots instead of bars. Stimulation with bars or gratings never evoked a different response than round dots or squares and was therefore not followed up even though it's widely used in other visual preparations such as mammalian V1 or LGN (Felsen et al., 2002;Mazer et al., 2002;Ringach et al., 1997).

For a linear cell, these measurements would not give great additional insight since one expects it to respond equally well to stationary and moving dots, furthermore the cell should not display differences in responses to dots moving in different directions. Additionally, in a linear system the spatial summing should be linear, that is a cell's response size scales up with the increase of the stimulus (size, intensity…). However, due to preprocessing in the retina and extensive interconnection within the brain, linear processing cannot be assumed for cells in the central visual system or in fact in any central

sensory system. A recent study of zebrafish tectal (PVZ) neurons in larvae showed that these neurons have increased calcium signals to moving spots than to stationary spots, most prominent when stimulated with small moving dots and respond less strong to stimuli increasing in size when flashed stationary(Niell and Smith, 2005).

In the present study of tectal neuropil neurons, a combination of many possible linear and nonlinear properties was observed. In Figure 21, averaged responses to a whole size query stimulus protocol are shown, starting with the responses to 10 stationary dots in the top row and the 4 moving directions below that. This cell responded with great preference to a moving stimulus as detected by comparing integrated response sizes for both stimuli (Figure 21b). Nevertheless the cell does respond readily to a presentation of a stationary spot and interestingly it prefers small spots over larger ones (Figure 21b right panel). The left panel of Figure 21b displays a stimulus response relationship that increases at first and then saturates at spot size 3-4 after which the response decreases again.
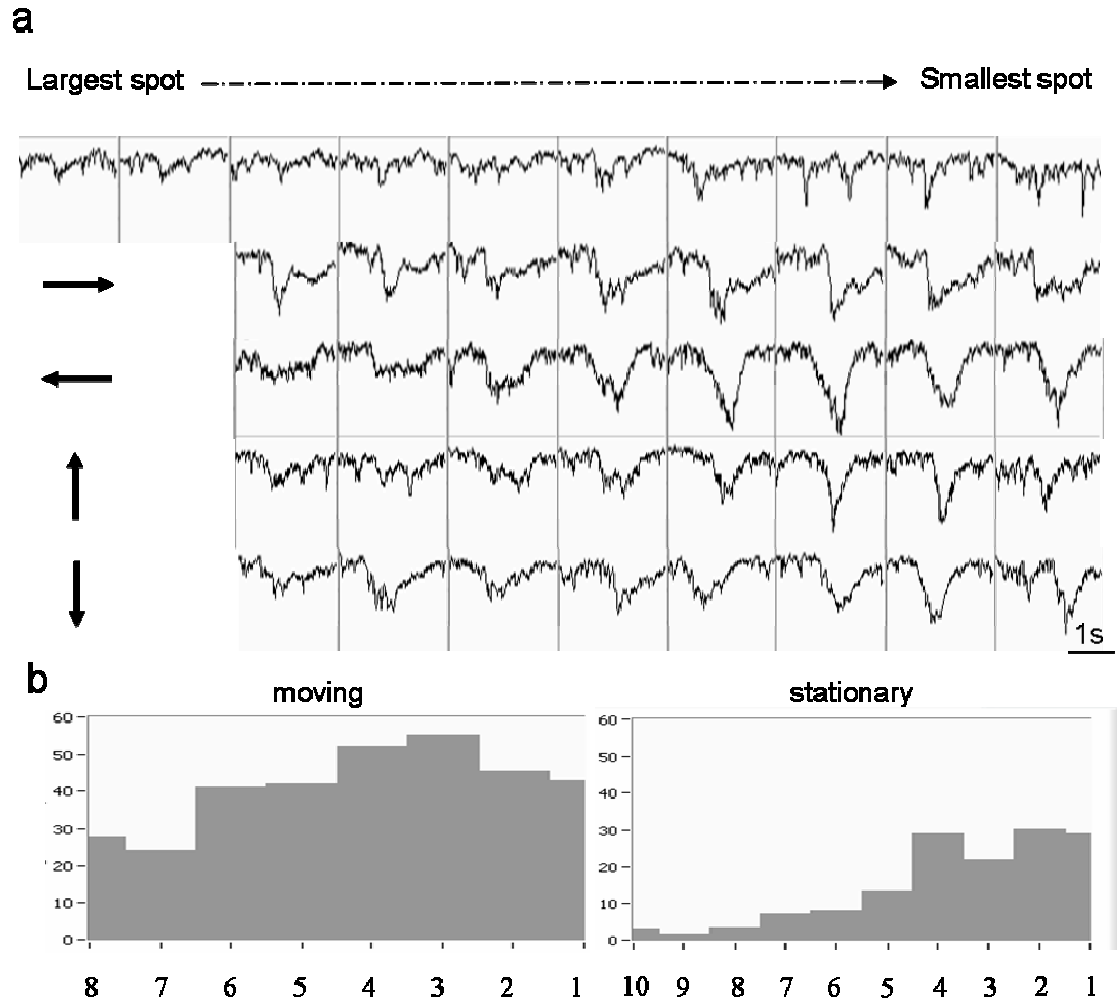
Figure 21: Responses to moving and stationary dots inside the RF
a: Each row displays the average response of 4 stimulus repetitions of stationary (top row) and moving dots (4 bottom rows, direction indicated by arrows). The responses to one direction (or stationary) are plotted in one row but were not shown in this order but randomly. Dot size is decreasing from left to right. The two biggest dots were only flashed stationary and not moved (9 and 10). In all 5 cases is the response size inversely correlated with the dot size. The quantification of the response size is shown in b. Each bar represents the relative response size in a time window (~500ms-1s) to a given spot size. Y-axis in arbitrary units. As in a, dot size deceases from left to right. The left panel shows relative response sizes to the preferred direction (left in a), the right panel for stationary dot presentation. A strong preference for moving dots can clearly be observed.

14 out of 20 analyzed cells responded more readily to moving spots when compared to stationary spots (or didn't respond to stationary stimuli at all), 4 responded with similar responses amplitudes to both stimuli, but never responded a cell better to a stationary spot.

In 2 cases the relationship of response size to stimulus type (stationary vs. moving) was dependant on the dot size: one cell that preferred bigger stimuli for both, stationary and moving dots, had equal response sizes for large dots, both moving and stationary. The responses to (less preferred) smaller dots however were bigger for moving spots than stationary spots which points out a higher sensitivity of the cell to moving dots. The second cell preferred small stationary dots but was size invariant for moving dots; the response size was similar for all cases except for a decreased response for big stationary dots. This is one example of non linear spatial summing, resulting in reduced response size to a larger stimulus.

For the stationary presentation, 12 out of 20 cells showed a roughly linear stimulus response relationship resulting in increasing response size with increasing spot size or a threshold response that would only occur after a certain size was reached. 4 cells responded size invariant, one cell only within a window of mid-size dots, 2 cells showed a preferred response to the small dots, one of them is shown in Figure 21b, and one cell didn't have a response to any size stationary dot but responded well to all sizes moving dots.

For the moving stimuli most cells responded roughly equally well to small and big dots (13 out of 20), 3 preferred big dots and 2 small dots (these were not the same cells that preferred small stationary dots).

Furthermore, 2 cells showed differences in size preference dependant on direction, that is one was size invariant ion one direction (up-down) and responded better to large dots for the other direction (left right). The other one was invariant for size in the left-right orientation but responded better to small spots when moved up and down.

Two more examples of stimulus-response relationships are shown in Figure 22. A moving stimulus elicited response sizes up to twice as large as stationary stimuli of the same size (cell A). For this cell a roughly linear spatial summing property was observed. Responses to larger spots consistently evoked larger responses than small spots for both cases. In the case of the stationary presentation a threshholded responses mechanism can be observed, where the cell only starts to respond once a given threshold of dot size is reached.

Even though none of the cells was purely selective for one direction, several cells showed a preferred direction which resulted in larger response amplitudes than all other directions. An example is shown in Figure 22 cell B, where one direction evokes twice the response amplitude than the opposite direction. The size dependency is different in both cases: for the preferred direction, an increase of the response occurs until saturation is reached (around size 5) beyond which no change in responses size happens, for the opposite direction the cell responds very much size independently. The two perpendicular directions evoked intermediate response sizes (not shown).

A preferred orientation of motion (either up/down or left/right) could be found in 12 out of 20 cells of which one showed a different preferred directions for small and big dots, respectively.
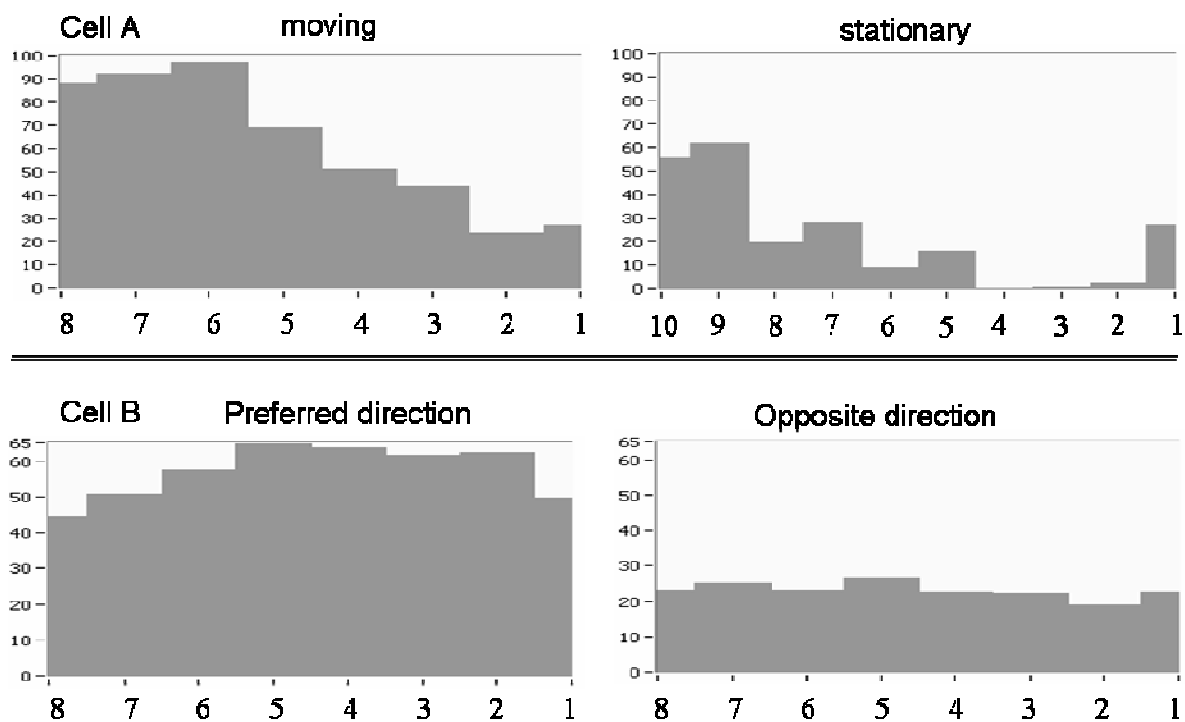
Figure 22: Quantification of response sizes for 2 different cells
Arrangement like in Figure 21b, spot size decreases from left to right, Y-axis in arbitrary units. Cell A: panels depict the integrated responses size in a given window to the preferred direction (left) and the stationary spot presentation (right). In this case the cell's responses increase with increasing spot sizes (moving). In the stationary case there is a threshold after which the cell starts responding (only the two largest dots). Cell B: both panel show integrated response sizes to moving stimuli, left for the preferred direction, right for the opposite direction. The preferred direction evokes a 2-3 fold increased response amplitude. The 2 direction of perpendicular orientation resulted in intermediate response values.

4.1.6 **RESPONSES TO NATURAL MOVIES**

The visual system is capable of detecting an enormous amount of different stimulus features and it would take many lifetimes to test them all and describe the responses they possibly evoke. Natural scenes can be used if one wants to test for complicated stimuli. The advantage of natural stimuli is of course that one can predetermine whether an animal can actually see them with tests for naturally occurring behaviors. Furthermore it is very satisfying to use stimuli that are relevant for the animal under natural conditions rather than highly artificial laboratory stimuli that will never in real life be actually seen by the animal, let alone be of any relevance to it. The disadvantage of natural visual scenes however, is that they are difficult to control and difficult to describe in their temporal and spatial content. A compromise is to simulate natural scenes and create stimuli that are very similar to behaviorally relevant stimuli but can be described in a computationally concise manner.

An example of such a simulated natural scene is shown in several frames in Figure 8. The movie shows moving images of paramecia, a natural prey for zebrafish larvae. The paramecia "swim" around and increase in size when they approach the position of the viewer (= the fish) and get smaller when they move the other way. Quick movements of the whole area simulate the fish's body movement; slow movements reflect the slower eye movement. These 2 types of movements can be observed in hunting larvae. The hunting/feeding behavior is almost stereotyped such that fish move their eyes with a prey and swim forward in short fast bursts that will result in the visual world passing by quickly (background movements).

30 cells could be recorded that reliably respond to several repetitions (at least 3) of the same movie. One example cell that responds reliably to different features within the natural-like movie is shown in Figure 23. A one minute voltage clamp recording (average of 3 trials) is shown in a. Several distinguishable responses are present. The single frames in b correspond to the sequence of movie that preceded the respective response, taking into account a retinal delay of about 100ms. This cell responds to small paramecia that move within the receptive field (left) as well as to one that increases in size while virtually approaching the fish (middle), and to a much larger paramecia that enters and moves about within the RF.
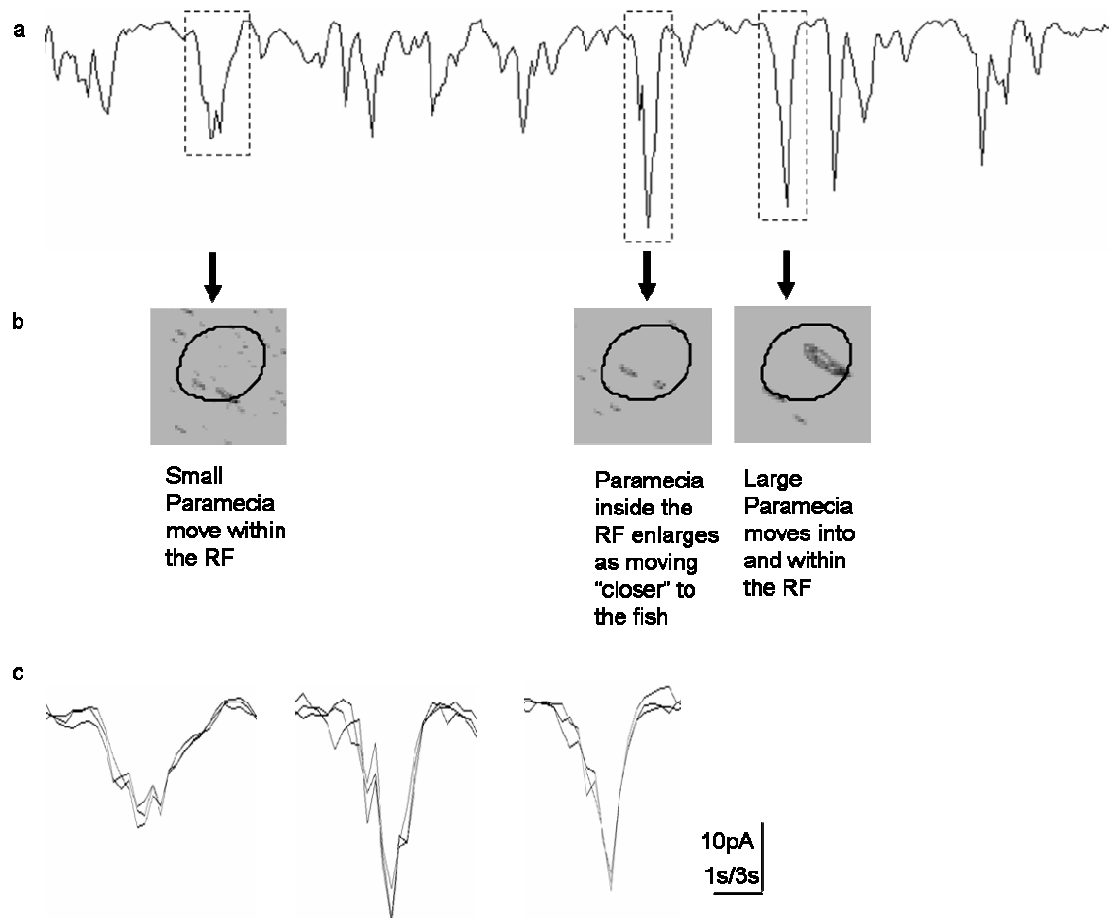
Figure 23: Responses to a natural-like movie
a: Average current trace of responses to 3 repetitions of the same movie sequence. b describes which features in the movie evoked the respective responses. c: magnification of all three current traces in a, individual sweeps are shown superimposed. Scale bar for the x-axis is 3s for a and 1s for c, the currents in a and c are equally scaled (10pA scale bar in c). The receptive field area is marked by the black circle.

Responses of the same cell presented in Figure 23 to a different movie are shown in Figure 24. Several large paramecia move inside the receptive field together and evoke a sustained response that lasts for about 10 seconds and is reproducible across several trials (a, right panel). As in Figure 23a single paramecia inside the receptive field evoke a more defined response also when many more are in close proximity of the receptive field boundaries (second response/movie frame in a/b). This prolonged response to a larger stimulus present inside the receptive field is consistent with the response to the mapping square of 25degrees (Figure 24c, grey bar), which also was as long as the stimulus presentation. In

the case of the moving paramecia the response also persists during the whole time the paramecia are present within the RF.
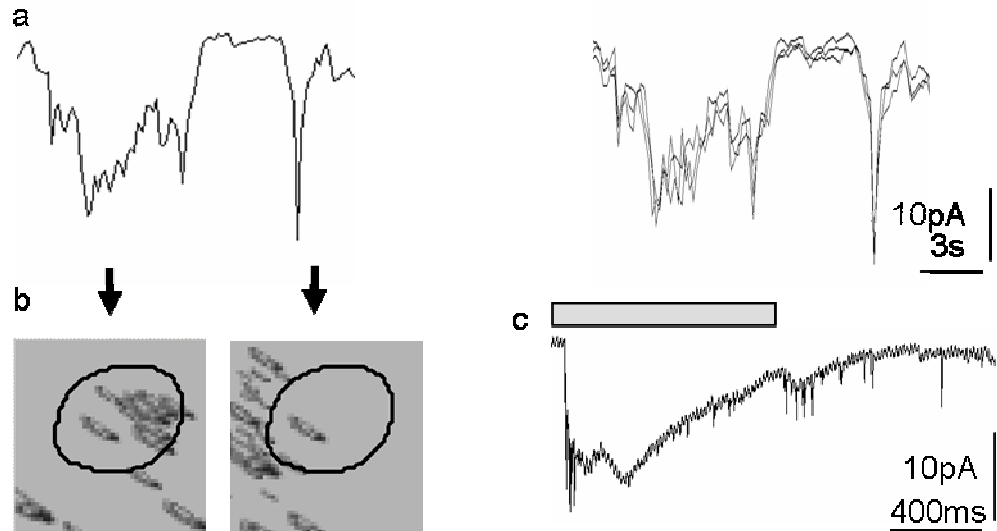
Figure 24: Different response types to different features in a movie
a shows the average current trace of responses to 3 repetitions of a natural-like movie (left) and the individual trials (right). The reproducibility is remarkable for both long compound and a fast response. b displays single movie frames that preceded the responses in a. Left: many large paramecia move within the area of the RF (black circle). They almost cover the entire RF area and evoke a sustained response whereas in the case for the right panel, a similar area covered by paramecia just outside the receptive field with only one left inside produce a defined and much faster response. c: average current trace of responses to 5 repetitions of stimulation inside the receptive field with a 25 degree square (mapping stimulus) results in a combination of transient and sustained responses.

4.2 MODELED RESPONSES

When trying to understand neuronal coding mechanisms it is helpful to model neuronal responses. The most challenging attempts try to model responses to highly complex stimuli, such as natural scenes. A relatively simple linear model can be used as a start to investigate neuronal deviations from linear processing. One can expect a good prediction for several aspects of a stimulus but on the other hand failures will occur, assuming that cells in the central nervous system don't process their inputs purely linearly. With the knowledge about when the linear model is insufficient to describe neuronal responses, one can go back to adjust the parameters of the initial model and include more complex algorithms in order to improve the prediction's ability to fit the data.

In the following sections different cases where the linear model fits the data well are presented.

4.2.1 SUCCESSFUL PREDICTIONS

Trying to model neuronal responses to a complex stimulus can require individual adjustments of the parameters or each given cell. In this study the evaluation of the prediction is weighed by the response reliability of the cell (standard deviation of the repeats to the mean response). Given a high trial to trial variability for any response, it is justifiable to weigh the predicted response at this point less than for responses that occur with high reliability. One can only expect any given model to predict the data well if the data is reproducible to a certain degree. Figure 25 displays the quantification of the response reliability (cross correlation value of different repeats).
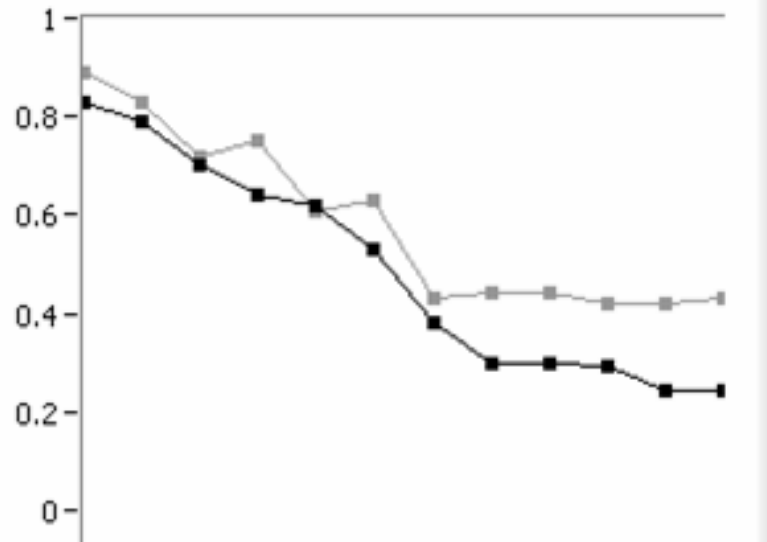
Figure 25: Response variability between repeated trials
Each data point represents the cross correlation value (y axis) for one cell (x-axis, total of 12 cells). The value is obtained by cross correlating all repetitions of one sweep (normalized to the autocorrelation). The cross correlation values obtained from unbinned data (see methods) are shown in black, points for binned data (10times) is shown in grey. Binning the data only increases the correlation value notably for cells with a lower response reliability (far right cells).

All the data is pre-binned to the frame rate of 60Hz at which the movie was shown. For cells with high response reliability, additional 10 fold binning of the data before the cross correlation has almost no effect on the correlation value (reliability of response) but for cells with high spontaneous activity, binning reduces some of this variability and therefore results in a better correlation value. To evaluate the prediction, the binning value was chosen to be 1 or 10 for each cell individually, depending which made a closer fit possible.

Generally, there is no relationship between the cross correlation value and the goodness of fit of the prediction. By altering the binning value one therefore doesn't introduce a general bias between cells. This independence of the prediction fit is illustrated in Figure 27. For 12 cells the r^2-value is sorted decreasingly (black points) and paired with the corresponding correlation quality of the single data repeats (grey bars). No relationship between goodness of fit and response variability could be observed. Cells with high r^2-direct values (left) show both high and low response variability. The best binning setting for each cell is summarized in Figure 26. For most of the cells binning had little effect on

60

the fit of the prediction, for 2 cells binning resulted in lower r^2-direct values and for 2 more cells it yielded a higher quality of fit.
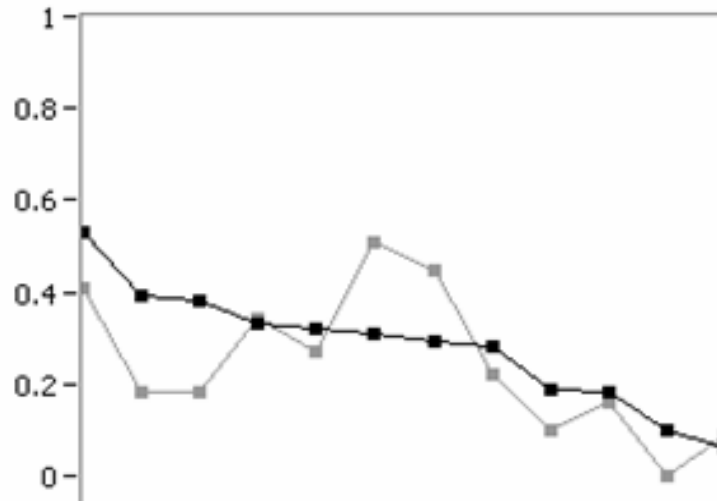
Figure 26: Best r^2-direct values result from different binning settings for different cells
R^2-direct values are shown for 12 cells in the case for unbinned data (black) and 10 times binned data (grey). For each cell a unique best binning option exists. The y-axis displays r^2-direct value. Individual cells are plotted on the x-axis.
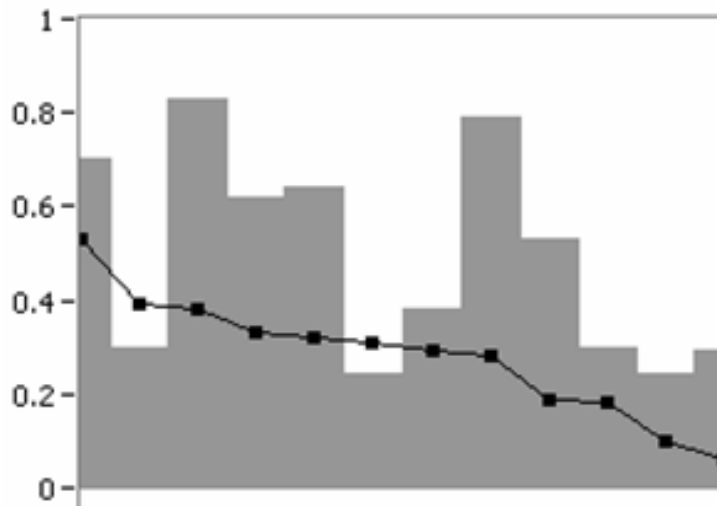
Figure 27: Quality of fit is independent of the response variability
The r^2-direct value is sorted (black) with the corresponding response variability in grey. High response reliability does not necessarily correspond to high r^2-direct values. The y-axis displays cross correlation value and r^2-direct value. Individual cells are plotted on the x-axis.

61

One further parameter was chosen individually to achieve the closest fit of the prediction to the data. For every cell it was determined whether a cylinder shaped or a divided spatial receptive field model (see methods) yields a better prediction fit.

Two examples where the model fits the data well are shown in Figure 28 and Figure 29. In both cases the model fits the larger responses in timing and amplitude well. In Figure 28, a cell with high spontaneous activity is shown (correlation between sweeps =0.42). The prediction was calculated with the uniform spatial receptive field model. This cell showed no preference for moving over stationary dots as determined with the moving/stationary dots stimulus. Thus, a division of the receptive field was not useful in order to predict the data better and to account especially for moving objects. The traces are binned by a factor of 10 to not erroneously decrease the prediction value by trying to predict noise (r^2-direct=0.51). All but one of the recognizable responses are fitted well. The model breaks down however, at positive response values because of the rectifying nature of the nonlinearity. It was assumed that only inward/negative responses would be elicited at a holding potential around -60mV.
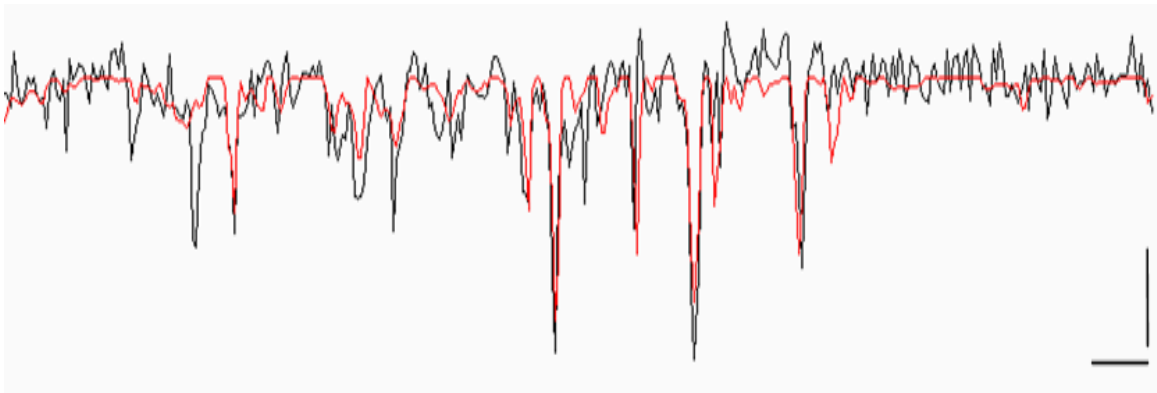
Figure 28: Predicted responses to a natural movie (cell A)
Average current trace of 6 repetitions (black) and predicted responses (red). The traces are binned 10fold to smooth over the high spontaneous activity of this cell (correlation coefficient 0.42). Responses visibly above noise are predicted well, both in timing and amplitude: r^2-direct=0.51. Scale bars: 3s, 5pA.

In a second example, the data allowed for unbinned comparison with the prediction in order to obtain the best fit: r^2-direct (=0.53). In this case, the best fit was achieved by using the divided spatial receptive field model that takes into account, when objects move within

the receptive field area. This is consistent with the observation that this cell preferred moving spots over stationary ones. The responses evoked by moving dots were up to 3 times higher than for stationary dots of comparable size.
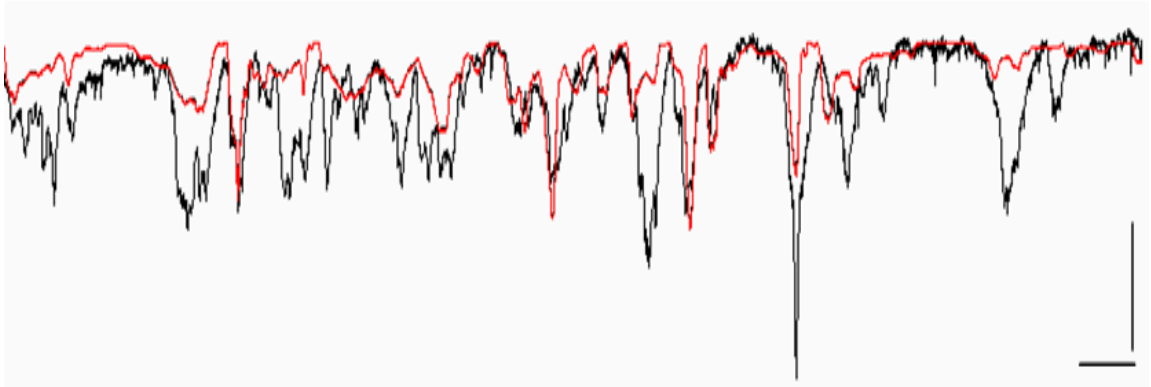

Figure 29: Predicted responses to a natural stimulus (cell B)
Average current trace of 6 repetitions (black) and predicted responses (red). The traces are unbinned because of low spontaneous activity of this cell (correlation coefficient 0.7). Many of the larger responses are fitted well: r^2-direct=0.53. Scale bars: 3s, 2.5pA.

Due to the different analysis of these two cells it is problematic to compare them directly. In the first case the prediction looks to fit the data better than in the second case, even though the fitting quantification yields a better value for cell B (Figure 29). Some of the recognizable responses in cell B are missed by the prediction, yet several responses are fit almost perfectly. The fact that this cell doesn't have a lot of spontaneous activity when no objects are shown increases the r^2-direct value because it "rewards" the model's capability to predict no response when no objects re shown. For a spontaneously more active cell the model would fail at these time points. These examples are very elucidating to display the importance of adjusting different parameters within a model, in order to achieve best prediction for two cells that behave differently.

4.2.2   **PREDICTION FAILURES**

Even though the prediction of responses to a natural movie is the most challenging and interesting test for a model, it is not necessarily the best to identify stimulus features where the model fails. The natural stimulus chosen was used because of its known behavioral relevance. It contains mostly moving elements of different sizes and directions but lacks stationary stimuli. To test specifically for the cells mechanisms of processing differences of stationary and moving stimuli, the model was challenged to predict responses to a sequence of interleafed moving and stationary dots of different sizes (see methods size query).

A requirement for a successful prediction with any model is that the cell responds with little variability. An advantage of the moving/stationary dot stimulus is that the cells responded more reproducibly to it compared to the natural stimulus. At all time points only one or no object is shown whereas in the movies a variety of objects are moving at most times.

The most remarkable response reliability of all cells is shown in Figure 30. Four repetitions of a stimulus extract o are shown at higher time resolution in Figure 30b. All 4 repetitions lie almost identically on top of each other. All sweeps were cross correlated with each other and normalized by the correlation value of each autocorrelation to obtain a correlation coefficient. The mean cross correllogram is shown in c. The correlation coefficient for this cell was 0.93 (the maximum possible value is 1).
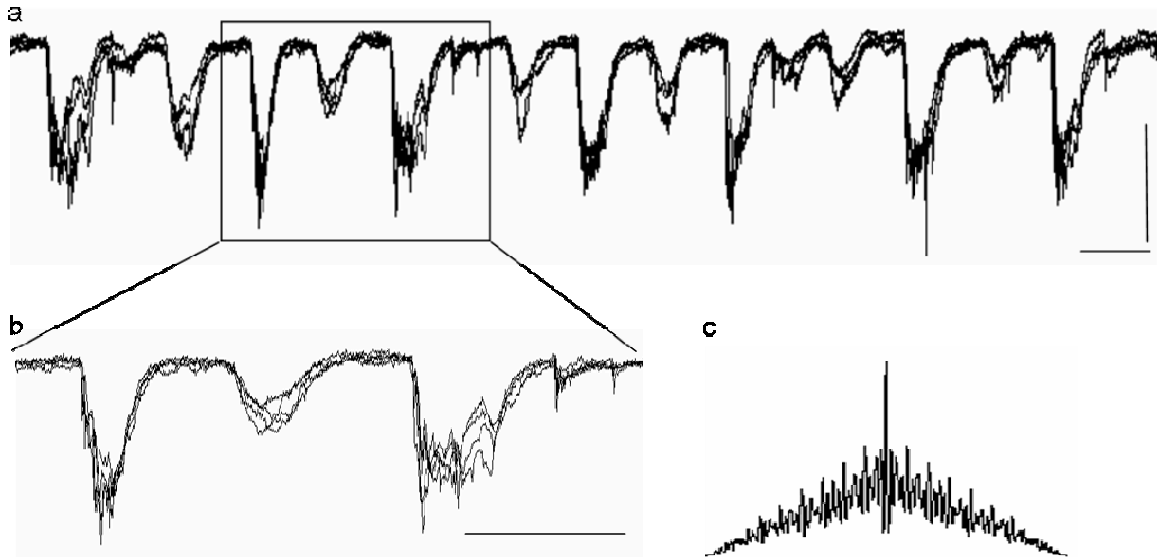
Figure 30: Reliability between repeated sweeps can be remarkably exact
An extract (~45s) from responses to a size query stimulus is shown. Dots of different sizes were flashed and moved in the receptive field. In a, 4 repetitions of the same sequence are shown overlaid (scale bars: 3s, 5pA). Responses in a are shown at higher time resolution in b. All 4 sweeps are strikingly similar (scale bar: 3s, 5pA as in a). In c the mean crosscorrellogram for all 4 sweeps is shown. A cross correlation factor of 0.93 was calculated for this cell (correlation for natural movie of this cell was 0.72).

Although this cell showed a remarkable response reliability, the model failed at several points to predict the responses. In Figure 31 the mean response of the extract as in Figure 30a is shown in black with the predicted responses superimposed in red. The timing of the response occurrence is fitted well in most cases but the response amplitude of the prediction doesn't match the data. Four examples are highlighted in the figure: the arrow above the responses indicates that a (small) moving dot evoked the response whereas the black dots indicate a stationary (larger) dot. In the case of the moving dots, the model dramatically under-predicts the response size. Contrarily, for the stationary dots the model predicts a response size that is much larger than the measured response.

In Figure 31b the response amplitudes of the measured data are sorted increasing from left to right (black) with the respective prediction values aligned accordingly in red. The left panel shows this analysis for the size query stimulus, the right panel for the natural movie. In this display it becomes more intuitive when the model fails to match the response amplitude. Whereas for small responses the model follows the trend of increase (with an

offset), it does not account for the larger data values. Instead, the large values are strongly under-predicted. Those high data values arise from moving stimuli. Naturally, a linear model doesn't distinguish between moving and static objects, but the cells often do. The analysis with a divided spatial receptive field model could in this case not account for the strong nonlinear behavior of this cell. The quantification of the motion preference is shown in c, where the grey bars show the relative response sizes to moving (left) and stationary (right) dots. The natural movie however, doesn't include such a wide range of object sizes and most of the time all objects are moving. The dramatic step in predicted response size does not occur (right panel Figure 31b).
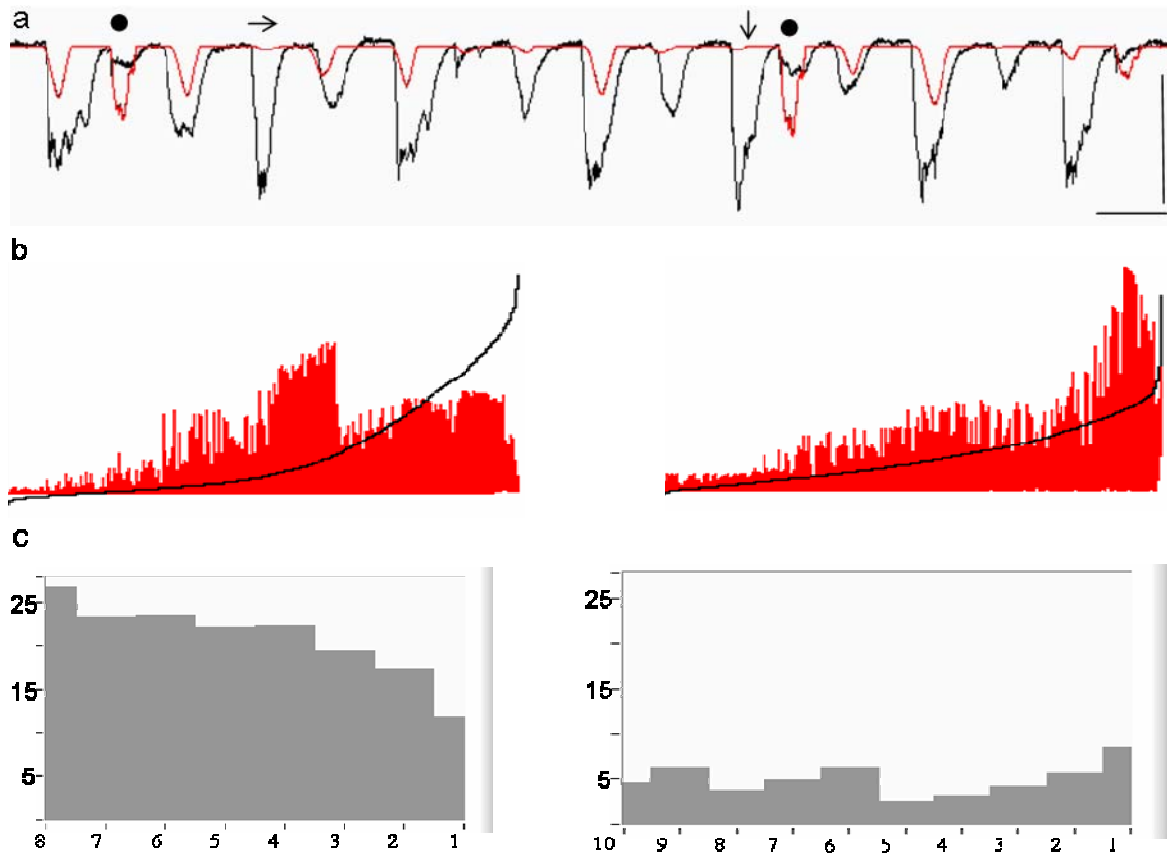
Figure 31: Prediction of responses to moving and stationary dots
a: The mean response of the same extract as in Figure 30 is shown in black, the predicted response is shown in red. The model is able to predict the response timing in most of the cases. However, deviations between the model and the data are striking in respect to response amplitude. The model dramatically under predicts events where a moving spot went through the receptive field (examples are marked by arrow above the responses) but over-predicts for stationary spots (examples are marked by dot above the responses). In b the response amplitude is sorted (black curve) and the corresponding prediction values are shown in red for the size query stimulus (left) and the natural movie (right). c: quantification of response sizes to moving (left) and stationary (right) dots. Dot size decreases from left to right within each panel, the y axis is given in arbitrary units to display relative differences.

r^2-direct in the case shown in Figure 31 was 0.38. This surprisingly high value for a prediction that misses the important responses can be explained by the nature of the stimulus. In the size query stimulus, several sequences occur between dots, when nothing is shown. A cell that remains silent between stimuli and has no spontaneous or dark/light tonic activity will obtain a better r2-direct value simply because the events when nothing happens are fitted well. In the case of the natural movie it is very rare that no objects are

67

shown. Therefore a high prediction value for the movie must be evaluated as more meaningful than the size query values which can be misleading.

Figure 32 shows the r^2- direct values for 2 different stimuli, a natural movie (grey) and the size query stimulation sequence (black) for all cells. The total values don't differ too much from each other across groups. However, under visual inspection it is clear that predictions fit the responses better for the movies than for the size query (see examples in the respective results sections). This demonstrates that absolute r^2- direct values must not be compared directly for stimuli that are very different. One conclusion to draw here however, is that the order of the values relative to each other within one group are not the same between groups, or in other words that the highest r^2-direct value is achieved for a different cell depending on the stimulus used to calculate it.
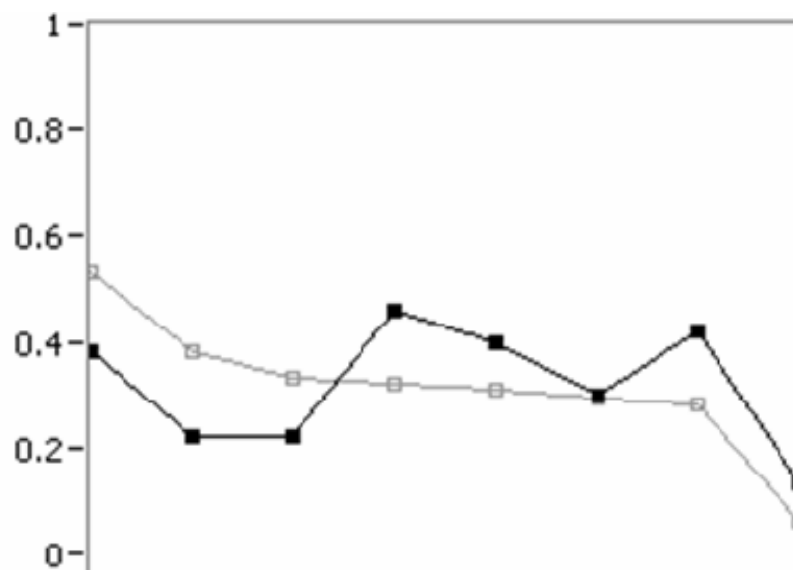
Figure 32: r^2-value for the prediction fit to the natural movie and size query stimulus
The r^2-direct value for the natural movie is sorted (grey) with the corresponding value for the same cell for size query stimulation in black. Note that the absolute values cannot be compared across groups due to the dramatic differences of the two stimuli. The conclusion that can be drawn is that different responses to different stimulus types are not predicted equally well within a group of cells The y-axis displays and r^2-direct value. Individual cells are plotted on the x-axis.

68

5   DISCUSSION

By developing a technique to record intracellularly *in vivo* while visually stimulating the larval zebrafish, this study aimed at describing responses of central visual neurons with an accuracy that could so far not be achieved with other methods of activity measurements, such as calcium imaging or extracellular recordings. The method of choice when aiming to study single cell physiology up to this day is still the use of an intracellular electrode, unfortunately many experimental drawbacks make this very difficult in several established model systems. Unlike in other animals like mice or cats, the surgery for *in vivo* patch clamp recordings in the zebrafish larvae are relatively easy, the animal stays alive without assistance such as perfusion of the gills, and cells can be recorded from for up to two hours. On the other hand it is also possible to collect data from a large number of animals in a relatively short time since the preparation of each animal only takes minutes and raising and keeping the larvae requires relatively little labor and space. In order to examine the effects of perturbations of any kind (genetic defects, behavioral or pharmaceutical manipulations) it is essential to have a general and comprehensive description of the visual system of healthy wildtype zebrafish. Knowing how a system works is of course crucial to detect failures and possibly find remedies to overcome them. Establishing the zebrafish visual system for reasonable high throughput intracellular electrophysiology will lead to a series of studies involving numerous mutants with alteration at different stages in the visual system. Descriptions that have so far been confined to genetics and anatomy can now include function to obtain a more complete picture about the vertebrate visual system. Since RGC regenerate after lesion this also allows for the investigation of functional reintegration of inputs after injury at the level of central nervous structures.

The first part of the present study offers a comprehensive description of receptive field properties of cells in the tectal neuropil of larval zebrafish. It is the first electrophysiology study in the larval central visual system and also the first study of neurons in the tectal neuropil, the entry site of retinal ganglion cell axons. Very few cell bodies are found within the neuropil (~10% of tectal neurons) and thus this region has so far been neglected. However, these neurons are very well accessible for *in vivo* patch clamp recordings and given their restricted number, different morphology, and specialized location within the

tectum, one could speculated that they have a different and more integrative function than the majority of tectal cells that are found within the PVZ.

The description of the cells' response characteristics includes spatial and temporal receptive fields and specific nonlinear properties such as motion and size selectivity. Roughly 1000 cells were recorded from to carefully extract useful stimulus parameters as well as obtain confidence that the cells in the neuropil are functionally a reasonably homogenous group. In the prediction study only a fraction of the latest experiments was included (12 cells) to ensure that all stimulus settings and set up configurations were comparable.

In the second part of the study this first description was evaluated by feeding the data into a model and comparing predicted responses of the cells with experimentally obtained responses. Identification of missing information will lead to further insight of how these cells compute their inputs and convert them into outputs that can lead to meaningful behaviors such as feeding. The possibility of being able to use a natural yet controllable stimulus is of great advantage over reduced artificial stimuli or natural stimuli that can be overwhelming in their complexity which makes interpretation of the data difficult and ambiguous. Additionally, it increases the relevance of this study because attempts to predict responses to stimuli with known behavioral relevance are so far lacking in the literature.

5.1   METHODOLOGICAL CONSIDERATIONS

The zebrafish visual system has so far mostly been studied under genetic aspects. Many mutations have been identified and anatomical studies revealed the respective defects; sometimes the defects could be linked with altered visual behaviors (Brockerhoff et al., 1995;Li, 2001;Neuhauss et al., 1999;Neuhauss, 2003). Many studies have also aimed at characterizing retinal physiology (Rinner et al., 2005a), (Brockerhoff et al., 1995;Brockerhoff et al., 1998), (Baier and Copenhagen, 2000), but up to this day, only a few groups have attempted to study the physiology of the central visual system in zebrafish (Niell and Smith, 2005;Sajovic and Levinthal, 1982a;Sajovic and Levinthal, 1982b).

However, considering that the zebrafish shows a variety of visually guided behaviors (Baier et al., 1996;Karlstrom et al., 1996b;Trowe et al., 1996)and is accessible for different methods of functional neuronal read out, it seems a very suitable model organism to undertake functional studies of the visual system.

Not all of the cells in the tectal neuropil of larval zebrafish are light responsive and the potential role of these neurons is unknown, but establishing the causes underlying this unresponsiveness was beyond the scope of this thesis.

Using reverse correlation methods has so far been widely established for spike trains in several sensory systems (Keat et al., 2001)and has recently been expanded to include sub-threshold membrane potential fluctuations; (Machens et al., 2004). The alteration to use EPSCs should in principle not be problematic; instead it allows for monitoring more information about the cell's responses since the information content in voltage clamp recordings is intrinsically higher than in extracellular or current clamp recordings. The stimulus waveform can equally well be convoluted with the current trace to obtain the receptive field. A potential greater computational effort is manageable for the data volumes employed in this study.

In order to measure the temporal and spatial receptive fields separately, it is crucial to determine whether the cells have space-time separable receptive fields. This was done in the very beginning of this study and was concluded to be the case. The space-time separability was measured with 2-diemnsional filtered noise, before adopting the separate measuring technique. Spatially filtered noise (instead of Gaussian white noise) was used to reduce the necessary recording time and care was taken to avoid undersampling the temporal or spatial response capabilities of the neurons. Inseparability means that a particular location in space cannot unambiguously be described as responding to 'on' or 'off' stimulation without including the temporal information. Classical space-time inseparable receptive fields are found, for example, in mammalian V1 simple cells (direction selective cells, (DeAngelis et al., 1993b;Reid et al., 1991). In the study presented here, cells were space-time separable, the 'on' and 'off' component of the receptive fields were widely overlapping and no strong direction selectivity was observed. Several cells however did show some preference for one direction or motion-orientation, these cells were then tested additionally in a separate experiment.

Since this is the first study in zebrafish using electrophysiology in combination with reverse correlation, several findings are difficult to validate and need to be put in perspective with studies of the visual system of other animals. Stimulating the cells with whole field light intensity fluctuations determined a strong preference for an 'off' stimulus for the majority of cells. With the 0.5 Hz whole field stimulations not a single cell was found that only responded to the light going 'on'. However, the reverse correlation analysis did extract pure 'on' moments. This seeming contradiction is explainable if the on response is slightly bigger then the off response and has the same temporal dynamics. It will then "win out" as the dominant structure in the reverse correlation analysis. The same problem can occur for the spatial measurements: the biggest responses will "win" over the smaller ones due to averaging. It was therefore useful in both cases, to stimulate the cells with slow visual stimuli additionally to the high frequency stimuli that were analyzed with reverse correlation. An example was given in Figure 20.

The choice of applying a linear model to cells in the central visual system was motivated by the necessity to obtain a first approximation of a description of these cells of any kind. Insights gained from this initial approach will be helpful to adjust model characteristics for following descriptions.

Since Hubel and Wiesel's first description of visual neurons (Hubel and Wiesel, 1959;Hubel and Wiesel, 1962) and hilariously reviewed in (Hubel and Wiesel, 1998), many groups who are studying the visual system are using bars and gratings to evoke neuronal responses and measure receptive fields, resolution limits, and contrast sensitivity in a number of visual areas. At the beginning of this study, an attempt was made to stimulate zebrafish tectal cells with black and white gratings of different contrasts and frequencies. Interestingly, gratings and bars turned out to be a rather bad stimulus for driving neuropil neurons and were therefore not used any further. Behaviorally, fish do see gratings however, they orient their swimming behavior accordingly or move their eye to follow the stripes (Maaswinkel and Li, 2003;Rinner et al., 2005b). This behavior however was shown to be independent of a functioning tectum and therefore it might be a segregated pathway within the fish visual system that specifically processes stripe-like stimuli.

To conduct a study in which a model is used to predict measured responses it is essential that a certain response invariability is given from trial to trial; otherwise any prediction attempt can only fail. A general feature of the nervous system seems to be that neurons in the sensory periphery can have machine-like reliability (Rieke and Baylor, 1998), whereas neurons in ascending areas often have more and more variable responses (Shadlen and Newsome, 1998). Kara et al. however have shown relatively low response variability for cells in the primary visual cortex, an area thought to have much higher trial to trial response variability (Kara et al., 2000). The functional hierarchical position of tectal neuropil cells needs yet to be determined, but anatomical observation strongly suggest that they receive direct inputs from retinal ganglion cells. Repeating the same stimulus sequence several times and cross correlating the individual traces showed that the criterion of high response consistency was given. In fact neurons in the neuropil can respond with a remarkable reproducibility of up to 93%.

5.2 SPATIAL RECEPTIVE FIELDS

Only two other studies of zebrafish tectal physiology are available to compare with the here presented results about spatial receptive fields. However, even though these studies were also conducted within the zebrafish optic tectum, both reports concentrate on cells in the larval (Niell and Smith, 2005) and adult (Sajovic and Levinthal, 1982b) PVZ, respectively and conclude nothing about neuropil neurons. Nevertheless, several general similarities can be noted between both groups of cells. Type I, S, T, and B cells were described by Sajovic and confirmed by Niell. I cells have no spontaneous dark activity and respond to light going 'on' and 'off' in a transient way. S cells have little dark spontaneous activity but respond in a sustained fashion to an 'on' stimulus. T cells fire tonically in the dark and have phasic 'on' and 'off' responses that are more prolonged than type I responses. All three cell types are highly motion sensitive. Cells with and without spontaneous dark activity that respond transiently to 'on' and/or 'off' stimuli were as well found in the tectal neuropil of zebrafish larvae. Type B cells however, are completely motion insensitive. Those were not found in the neuropil but do exist in the PVZ of both, larval and adult zebrafish.

Consistent with Niell et al, who found that larval PVZ neurons don't display spatial refinement of their receptive fields during the observed period between onset of vision and 9-11dpf, the spatial extend of the receptive fields of neuropil cells presented here also does not change (average RF size at 4dpf was 18° and 18.75°at 10dpf). One might have expected functional changes in the form of spatial refinement, because during the first week of development a morphological refinement of retinal axons is taking place (Gnuegge et al., 2001), which could potentially lead to a functional alteration.

The phenomenon of negative spatial summing has been observed in the optic tectum of adult and larval fish as well as in the superior colliculus of higher vertebrates (Pinter and Harris, 1981) and could also be detected in the neurons tested in the present study. It results in an optimal neuronal response to an object smaller than the receptive field size and a decreasing response to larger objects. In the neuropil, 4 out 20 cells showed negative spatial summing, 2 cells for stationary, and 2 for moving spots respectively.

Differences between PVZ cells and neuropil neurons are discussed in the following paragraphs (they all refer to the studies of Niell and Sajovic, respectively). Both PVZ studies report a retinotopic organization of receptive fields of tectal cells which could not be found for cells in the neuropil. The basis for this phenomenon might lie in the difference in the anatomy of both brain areas and the different morphology of the neurons within. PVZ cells show a very stereotype morphology: a major unipolar dendritic trunk arises from the cell body and enters the superficial layers parallel to its neighboring cells resulting in a ladder-like structure(Naumann E.A. and Engert F., 2005). On the other hand, cells in the neuropil are often bipolar and their dendritic trees can extend over large areas along the rostro caudal axis. Given that retinal axons enter the tectum in an organized way such that the temporal and nasal retinal fibers project to the rostral and caudal tectum, respectively, one could speculate that the large dendritic extension along the rostro-caudal axis might lead to a loss of retinotopy due to dendritic integration of several inputs from different locations of the retina.

Receptive fields of larval tectal neuropil cells reported in the present study had a mean area of 17° (+/-10°) when measured with an 'off' stimulus and 14° (+/-10°) for the 'on' stimulus which is smaller than reported in either of the PVZ studies. Niell reported receptive field sizes for larval PVZ neurons with a mean of 40° and Sajovic measured

almost similarly large receptive fields for cells in the adult PVZ (34°). Considering that the cells studied in this present work were all recorded from the cells in the tectal neuropil and were therefore lying within the RGC axonal entry zone (where smaller receptive fields (~10°) can be measured from axons (Sajovic and Levinthal, 1982b)) the discrepancy of receptive field size measured in this study compared to the other two seem complimentary rather than contradicting.

A divided structure of receptive fields (compound RFs) was reported for adult PVZ cells by the same group whereas in larval neuropil cells the receptive fields were always continuous. This might result from higher levels of background illumination in the experiments here since most receptive fields were measured with a dark spot on a light background. Background illumination was reported to decrease or extinguish accessory receptive fields. Even in the cases when the receptive field was measured at opposite contrast (white square on black background), the background was never totally dark due to the background illumination of the projector.

For the cells presented here, the spatial extend of the 'on' and 'off' receptive fields were widely overlapping but the 'off' RF usually extended to a larger area. The opposite was found to be the case in the adult PVZ cell where the 'on' response was usually dominant. The fact that the 'on' and 'off' receptive field area overlapped to the described extend is interesting. Cells in the early visual system like the retina or retino-recipient structures, have been described with center surround receptive fields. Receptive fields where excitatory and inhibitory sub-regions are not segregated are more commonly found in higher visual processing areas. The classical example of such neurons are complex cells in the primary visual cortex described by Hubel and Wiesel in the early 1960s.

5.3   TEMPORAL RESPONSE CHARACTERISTICS

In the characterization performed by Sajovic and later confirmed by Niell a cell group was described that responded only to sustained decrease of light with ongoing activity (type-S cells). Cells with purely sustained responses could not be observed in zebrafish neuropil. In all cases at least one of the stimulus transitions ('on' or 'off') lead to a transient response.

Different amounts of sustained, stimulus dependant activity, either during dark or light periods were always observed on top of that, but never exclusively.

Nothing had so far been known about the temporal receptive fields of zebrafish tectal neurons. Temporal receptive fields have been described with white noise analysis in a variety of species and visual brain structures though (for review see (Ringach, 2004)), including cat lateral geniculate nucleus (LGN) and visual cortex (Cai et al., 1997;De Valois et al., 2000;Worgotter et al., 1999)

Neurons in the LGN typically display a biphasic temporal moment. Maturation leads to more cells with biphasic moments at older ages (Cai et al., 1997). This maturation however happens rather late, at least when compared with the timing of maturation of the spatial receptive field parameters. Whereas at the age of 4 weeks little changes occur in the spatial organization of LGN receptive fields in kittens, substantial modifications are still taking place with respect to temporal profiles in LGN as well as striate cortex neurons (DeAngelis et al., 1993a).

In the light of the information about cat LGN development, analysis of the temporal moments with respect to their biphasicness was performed for larval neuropil cells over different age groups. The number of cells with biphasic moments was compared to the monophasic moments at each day and the extent of the biphasicness was monitored, that is different thresholds were set to determine whether a cell was considered biphasic or not (see methods). In the zebrafish larval neuropil 45% of all measured cells between day 3 and 11 had a biphasic moment as measured with whole-field flickering calculated with reverse correlation techniques. The percentage of biphasic cells increased significantly between day 3 and day 10. Whether this is a generally valid trend need s to be investigated further since a smaller percentage of biphasic cells was observed for the 11 day old group.

The relative contribution of 'on' cells to the population showed a significant increase over the observed developmental period. Starting with more 'off' cells as determined by the mean deflection of the moments cells undergo a change that results in more 'on' cells after day 9. Whether this is due to different maturation of the separate pathways from the retina or comes about by computational changes on the tectal cell or a rearrangement of axonal arbors of RGCs is open for speculation.

5.4   **SIZE AND MOTION QUERY**

A separate stimulus protocol was designed specifically to inquire about the cells' response properties in respect to moving objects. Dots of different sizes and directions were presented in the receptive field and the responses were analyzed with respect to spatial summing and direction selectivity. These characteristics were also compared to responses evoked by stationary stimuli of comparable sizes.

The most obvious finding was that in 14 out of 20 cells a moving dot consistently evoked a larger response than a stationary dot of the same size. Two cells showed exceptional behavior that is described in detail in the result section 4.1.5. Briefly, one cell was invariant to motion for large objects, while it responded preferentially to small moving objects. The second cell was size invariant for moving objects and did show a preference for small over large objects when presented stationary. Even though this size invariance for moving stimuli was categorized before for neurons in the PVZ, it is difficult to draw conclusions for the present cell group since this behavior was only observed in one out of 20 cells and can therefore not be used to establish a cell group.

The categorization of tectum cells into 4 functional groups was established first by Sajovic and later confirmed by Niell (Niell and Smith, 2005;Sajovic and Levinthal, 1982a;Sajovic and Levinthal, 1982b). It describes two groups that respond strongly to moving stimuli and are distinguished from each other by the presence or absence of direction selectivity, a third group that is insensitive to motion, and finally a fourth cell group that only responds to a sustained decrease in light intensity. This was found to be different for cells in the larval neuropil. Most striking is the absence of direction selectivity and motion insensitivity. Classic direction selectivity, where one direction evokes the largest response and the opposite (180°) results in a dramatically reduced or no response, could not been detected in the neuropil. A moderate preference for one direction could be observed for neuropil cells. Furthermore, this preference was often valid for one orientation of movement over the perpendicular orientation, rather than for one single direction. In addition, type B cells, which are completely insensitive to moving stimuli, were found in adult and larval PVZ neurons but not in neuropil cells. In fact, all cells responded at least equally well or better to moving stimuli than to static stimuli. These two

contradicting findings might simply be attributable to the fact that the data was collected in different functional subgroups of the optic tectum.

5.5   NATURAL MOVIES

The presentation of simulated natural movies rather than real movies was motivated by several reasons: one advantage was that filming paramecia in a dish resulted in a very noisy movie with uncontrollable dirt moving around and background changes of the illumination which resulted in less reliable response reproducibility from trial to trial. The jerky background movement (fish turning) and slow movements (fish rotating the eyes) were difficult to implement into a filmed movie but were included in the simulation. Furthermore one cannot steer the real paramecia to control their position within the visual field.

Most cells presented with the simulated natural movie responded well and reliable. The consistency with which the cell responded to objects moving in an out of their receptive fields is clear evidence that the responses were stimulus evoked.

5.6   EVALUATION OF THE MODEL

The goal of modeling neuronal responses to any stimulus is to obtain a compact description of a neuron in order to understand the mechanisms that govern information encoding. In order to successfully predict responses it is necessary that a neuron will reliably respond in the same way in repeated trials of the same stimulus presentation. Many studies therefore concentrate on neurons in the early visual system which can display a remarkable response invariability (Reich et al., 1997), (Berry et al., 1997), (Berry and Meister, 1998), (Kara et al., 2000;Reinagel and Reid, 2000).

A few years ago Keat et al were able to fit data recorded from different types of ganglion cells as well as cat LGN cells to a "0-diminsional" stimulus remarkably well. The parameters of their linear model were adjusted for each cell individually to account for the correct onset and number of spikes. By additionally including a negative feedback

mechanism and two separate noise injectors they were able to fit the data within the natural limits of trial to trial variability (Keat et al., 2001).

Several differences between the study presented here and Keat's approach can explain why this same high level of fit acuity could not be reached here: most striking is that they used a "0-dimensional" stimulus with no spatial component. The higher complexity of a stimulus varying in space and time makes the correct prediction much harder and can therefore easily lead to a less accurate fit. In fact, in their conclusion Keat et al end with the suggestion that predicting responses to a two-dimensional or even a natural stimulus would be the ultimate goal. The fact that current traces were used instead of spikes accounts for an additional increase of complexity. The information included in current traces is inherently higher than that in spikes because spikes arise through thresholding. If one wants to predict sparsely occurring spikes it is easier to fit them precisely because of the digital nature of spikes: they can be described by only one parameter, the time point of their occurrence. On the other hand, when one wants to fit spike trains with different firing rates the situation is more complicated due to the fact that the number of spikes needs to be translated into an amplitude and a duration. A probability distribution is calculated that can be viewed as an 'analog version of a spike train'. This will look almost identical to the current traces used here. One needs to fit the "when" and include two separate parameters for amplitude and duration, respectively and indeed, in Keat's study the prediction algorithm had to be adjusted (e.g. addition of negative feedback mechanism) to account for denser occurring spikes. When looking at the data shown here, one can clearly recognize that it is also the prediction of the correct amplitude where the model fails. The timing and duration are both rather well accounted for in the predictions of the natural movies and for the size query sequence. The linear model simply misses the changes in amplitude for responses to different dots that occur due to a motion preference found in these cells and in some cases due to non-linear spatial summing properties.

The problem of wrongly predicting the magnitude of events can be observed as well in studies concerned with spike trains that include bursts because spike bursts can be regarded as a non-linear amplification within the response (Lesica and Stanley, 2004).

The under- or over-prediction of non-linear responses is of course not limited to studies in the early visual system. In the auditory cortex Machens et al were able to predict

the general timing of the occurrence of sub-threshold membrane potential fluctuations to natural stimuli but their model also collapsed with respect to the precise amplitude of responses (Machens et al., 2004).

It seems that generally the overall strength of a response is the most difficult parameter to predict correctly, whether it's the amplitude of an analog signal, or the increased magnitude expressed as a burst of spikes. To further progress in predicting non-linear neurons, the concept of linear models needs to be expanded or altogether changed. Neural network models are becoming more and more prominent in improving predictions where linear models fail (Lau et al., 2002). However, the computational complexity goes far beyond the scope of this thesis.

5.7 PLACING TECTAL NEUROPIL CELLS WITHIN THE HIRARCHY OF THE VISUAL SYSTEM

Anatomically, cells in the tectum are comparable to cells in other retino-recipient areas, such as the LGN or the superior colliculus in mammals.

The LGN has long been regarded as a mere (largely passive) relay station between retina and visual cortex. Only in the last 10 years has it become clearer that the LGN actually actively shapes the visual signals on their way to the visual cortex. This notion is of course problematic to adapt for the fish brain since teleosts don't have a cortex and the tectum is generally viewed as the mayor visual processing center in the teleost brain. Another anatomical difference lies in the different layering of these two structures: whereas LGN cells are layered according to which eye they arise from, the optic tectum only receives direct inputs from the contralateral eye. LGN cells as well as retinal ganglion cells in many vertebrates show a center surround structure. These types of receptive fields could not be isolated specifically here, but the finding of negative spatial summing indicates related properties.

The superior colliculus in mammals is involved in controlling eye movements and its neurons are known to receive information about moving objects(monkey: Cynader and Berman, 1972;cat: Hoffman, 1973;hamster: Mooney et al., 1985). Experiments in fish, in

which the optic tectum was ablated showed that simple visual behaviors such as the OKR and OMR were not dependant on a functional tectum. This implies that the tectum cannot be responsible for all movement detection and that tectum independent brain areas are responsible for these less complex visual behaviors (Roeser and Baier, 2003). Prey capture on the other hand was compromised with an ablated tectum (Gahtan et al., 2005;Roeser and Baier, 2003). Overall this indicates that the cells in the optic tectum can also not be generalized to "replace" the superior colliculus of mammals.

Generally this would mean an overall "downshift" of the visual hierarchy as compared to mammals due to the lack of a cortical structure at the highest end, assuming the tectum is indeed responsible for the more sophisticated processing tasks and that classical midbrain areas in mammals like LGN and SC could functionally be equated with extratectal nuclei, for example the pretectum.

The receptive field properties of cell in the tectal neuropil cannot easily be sorted into existing categories of other animals because they show manifold similarities with cells throughout different hierarchical stations in the visual system. Regarding the temporal aspects, the cells with biphasic moments resemble retinal as well as higher neurons. Triphasic moments on the other hand have been described for mammalian cortical cells with space time inseparable receptive fields (simple cells).

The spatial overlap of 'on' and 'off' receptive field areas has been extensively described for complex cells in the visual cortex, however an orientation tuning is lacking in the tectal cells nor are they particularly direction selective. A similar overlap of different regions was described for frog and squirrel ganglion cells but instead of 'on' and 'off' receptive fields these cells responded equally well to two different color channels in overlapping position (Michael, 1968). The observed receptive fields and temporal patterns suggest that the cells in the neuropil of the optic tectum are functionally more similar to higher visual processing centers in other vertebrates than their anatomical correlates like the LGN or SC.

Unlike any of the mentioned structures in higher vertebrates or within the fish tectum, cells in the tectal neuropil do not show a retinotopic organization. This makes them a unique group of neurons within the visual system of fish. Within other vertebrate visual systems however it is a general feature that the higher the cells lie in the hierarchy, the less retinotopy they display.

81

6   CONCLUSION

The zebrafish is a well established model system for genetic and anatomic studies of the vertebrate visual system but up till now an electrophysiological approach to investigate functional properties of larval optic tectum neurons had been missing. The establishment of an *in vivo* patch clamp preparation described in this thesis contributes to the understanding of visual processing. A comprehensive description of neuronal coding mechanisms is given and tested with a linear model.

Cells in the neuropil of the optic tectum process visual stimuli within a restricted area of the visual field and specific temporal properties. In the first 8-9 days after hatching, more cells have 'on' moments as determined with reverse correlation technique. In the following 3 days this is reversed and cells with 'off' moments prevail. During the same time, more and more cells with biphasic moments emerge. All cells respond preferentially to moving object such as paramecia, which were used as a natural stimulus. Several non-linear properties like negative spatial summing and an orientation preference suggest that a fair amount of processing is occurring in these neurons. Modeling neuronal responses to a natural stimulus with a linear model yielded good fits of the data in many cases but failed in others.

A lot of insight was gained with the help of the data and methods presented here and a new series of investigations can now follow, including characterization of mutants and improvements of the model.

Reference List

1. Baier,H. and Copenhagen,D. (2000). Combining physiology and genetics in the zebrafish retina. J.Physiol 2000.Apr 1;524.Pt.1:1. *524 Pt 1*, 1.

2. Baier,H., Klostermann,S., Trowe,T., Karlstrom,R.O., Nusslein-Volhard,C., and Bonhoeffer,F. (1996). Genetic dissection of the retinotectal projection. Development *123*, 415-425.

3. Bair,W. (2005). Visual receptive field organization. Curr.Opin.Neurobiol.2005.Aug.;15.(4):459.-64. *15*, 459-464.

4. Berry,M.J. and Meister,M. (1998). Refractoriness and neural precision. Journal of Neuroscience *18*, 2200-2211.

5. Berry,M.J., Warland,D.K., and Meister,M. (1997). The structure and precision of retinal spike trains. Proc.Natl.Acad.Sci.U.S.A *94*, 5411-5416.

6. Brockerhoff,S.E., Dowling,J.E., and Hurley,J.B. (1998). Zebrafish retinal mutants. Vision Research *38*, 1335-1339.

7. Brockerhoff,S.E., Hurley,J.B., Janssen-Bienhold,U., Neuhauss,S.C., Driever,W., and Dowling,J.E. (1995). A behavioral screen for isolating zebrafish mutants with visual system defects. Proc.Natl.Acad.Sci.U.S.A *92*, 10545-10549.

8. Bruce,C., Desimone,R., and Gross,C.G. (1981). Visual properties of neurons in a polysensory area in superior temporal sulcus of the macaque. J.Neurophysiol. *46*, 369-384.

9. Cai,D., DeAngelis,G.C., and Freeman,R.D. (1997). Spatiotemporal receptive field organization in the lateral geniculate nucleus of cats and kittens. J.Neurophysiol. *78*, 1045-1061.

10. Chichilnisky,E.J. (2001). A simple white noise analysis of neuronal light responses. Network.2001.May.;12.(2):199.-213. *12*, 199-213.

11. Cynader,M. and Berman,N. (1972). Receptive-field organization of monkey superior colliculus. J.Neurophysiol. *35*, 187-201.

12. Dayan,P. and Abbott,L.F. (2001). Theoretical Neuroscience. MIT Press).

13. de Boer,E. and Kuyper,P. (1968). Triggered correlation. IEEE Trans Biomed Eng *15*, 169-179.

14. De Valois,R.L., Cottaris,N.P., Mahon,L.E., Elfar,S.D., and Wilson,J.A. (2000). Spatial and temporal receptive fields of geniculate and cortical cells and directional selectivity. Vision Res.2000.;40.(27.):3685.-702. *40*, 3685-3702.

15. DeAngelis,G.C., Ohzawa,I., and Freeman,R.D. (1993a). Spatiotemporal organization of simple-cell receptive fields in the cat's striate cortex. I. General characteristics and postnatal development. J.Neurophysiol. *69*, 1091-1117.

16. DeAngelis,G.C., Ohzawa,I., and Freeman,R.D. (1993b). Spatiotemporal organization of simple-cell receptive fields in the cat's striate cortex. II. Linearity of temporal and spatial summation. J.Neurophysiol. *69*, 1118-1135.

17. DeAngelis,G.C., Ohzawa,I., and Freeman,R.D. (1995). Receptive-field dynamics in the central visual pathways. Trends in Neuroscience *18*, 451-458.

18. Easter,S.S., Jr. and Nicola,G.N. (1996). The development of vision in the zebrafish (Danio rerio). Dev.Biol. *180*, 646-663.

19. Engert,F., Tao,H.W., Zhang,L.I., and Poo,M.M. (2002). Moving visual stimuli rapidly induce direction sensitivity of developing tectal neurons. Nature *419*, 470-475.

20. Felsen,G., Shen,Y.S., Yao,H., Spor,G., Li,C., and Dan,Y. (2002). Dynamic modification of cortical orientation tuning mediated by recurrent connections. Neuron *36*, 945-954.

21. Gahtan,E., Tanger,P., and Baier,H. (2005). Visual prey capture in larval zebrafish is controlled by identified reticulospinal neurons downstream of the tectum. J.Neurosci.2005.Oct.5;25.(40.):9294.-303. *25*, 9294-9303.

22. Gnuegge,L., Schmid,S., and Neuhauss,S.C. (2001). Analysis of the activity-deprived zebrafish mutant macho reveals an essential requirement of neuronal activity for the development of a fine-grained visuotopic map. Journal of Neuroscience *21*, 3542-3548.

23. Guo,S. (2004). Linking genes to brain, behavior and neurological diseases: what can we learn from zebrafish? Genes Brain Behav. *3*, 63-74.

24. Hamill,O.P., Marty,A., Neher,E., Sakmann,B., and Sigworth,F.J. (1981). Improved patch-clamp techniques for high-resolution current recording from cells and cell-free membrane patches. Pflugers Arch. *391*, 85-100.

25. hoffman,K. Conduction velocity in pathways from retina to superior colliculus in the cat: a correlation with receptive field properties. Journal of Neurophysiology 36:409-424. 1973.
Ref Type: Generic

26. Hubel,D.H. and Wiesel,T.N. (1959). Receptive fields of single neurones in the cat's striate cortex. J.Physiol *148*, 574-591.

27. Hubel,D.H. and Wiesel,T.N. (1962). Receptive fields, binocular interaction and functional architecture in the cat's visual cortex. J.Physiol *160*, 106-154.

28. Hubel,D.H. and Wiesel,T.N. (1998). Early exploration of the visual cortex. Neuron *20*, 401-412.

29. Jones,J.P. and Palmer,L.A. (1987). The two-dimensional spatial structure of simple receptive fields in cat striate cortex. J.Neurophysiol. *58*, 1187-1211.

30. Kara,P., Reinagel,P., and Reid,R.C. (2000). Low response variability in simultaneously recorded retinal, thalamic, and cortical neurons. Neuron 2000.Sep.;27.(3):635.-46. *27*, 635-646.

31. Karlstrom,R.O., Trowe,T., Klostermann,S., Baier,H., Brand,M., Crawford,A.D., Grunewald,B., Haffter,P., Hoffmann,H., Meyer,S.U., Muller,B.K., Richter,S., van Eeden,F.J., Nusslein-Volhard,C., and Bonhoeffer,F. (1996a). Zebrafish mutations affecting retinotectal axon pathfinding. Development *123*, 427-438.

32. Karlstrom,R.O., Trowe,T., Klostermann,S., Baier,H., Brand,M., Crawford,A.D., Grunewald,B., Haffter,P., Hoffmann,H., Meyer,S.U., Muller,B.K., Richter,S., van Eeden,F.J., Nusslein-Volhard,C., and Bonhoeffer,F. (1996b). Zebrafish mutations affecting retinotectal axon pathfinding. Development *123*, 427-438.

33. Keat,J., Reinagel,P., Reid,R.C., and Meister,M. (2001). Predicting every spike: a model for the responses of visual neurons. Neuron *30*, 803-817.

34. Lau,B., Stanley,G.B., and Dan,Y. (2002). Computational subunits of visual cortical neurons revealed by artificial neural networks. Proc.Natl.Acad.Sci.U.S.A *99*, 8974-8979.

35. Lesica,N.A. and Stanley,G.B. (2004). Encoding of natural scene movies by tonic and burst spikes in the lateral geniculate nucleus. Journal of Neuroscience *24*, 10731-10740.

36. Li,L. (2001). Zebrafish mutants: behavioral genetic studies of visual system defects. Dev.Dyn.2001.Aug.;221.(4):365.-72. *221*, 365-372.

37. Maaswinkel,H. and Li,L. (2003). Spatio-temporal frequency characteristics of the optomotor response in zebrafish. Vision Res.2003.Jan.;43.(1):21-30. *43*, 21-30.

38. Machens,C.K., Wehr,M.S., and Zador,A.M. (2004). Linearity of cortical receptive fields measured with natural sounds. Journal of Neuroscience *24*, 1089-1100.

39. Mancini,M., Madden,B.C., and Emerson,R.C. (1990). White noise analysis of temporal properties in simple receptive fields of cat cortex. Biological Cybernetics *63*, 209-219.

40. Marmarelis,V.Z. (1991). Wiener analysis of nonlinear feedback in sensory systems. Ann.Biomed.Eng *19*, 345-382.

41. Marmarelis,V.Z. (2004). Nonlinear Dynamic Modeling of Physiological Systems. Wiley-IEEE Press Series on Biomedical Engineering).

42. Martinez,L.M., Wang,Q., Reid,R.C., Pillai,C., Alonso,J.M., Sommer,F.T., and Hirsch,J.A. (2005). Receptive field structure varies with layer in the primary visual cortex. Nat.Neurosci.2005.Mar.;8.(3):372.-9.Epub.2005.Feb.13. *8*, 372-379.

43. Mazer,J.A., Vinje,W.E., McDermott,J., Schiller,P.H., and Gallant,J.L. (2002). Spatial frequency and orientation tuning dynamics in area V1. Proc.Natl.Acad.Sci.U.S.A 2002.Feb.5;99.(3):1645.-50.Epub.2002.Jan.29. *99*, 1645-1650.

44. McLean,J., Raab,S., and Palmer,L.A. (1994). Contribution of linear mechanisms to the specification of local motion by simple cells in areas 17 and 18 of the cat. Vis.Neurosci. *11*, 271-294.

45. Mechler,F. and Ringach,D.L. (2002). On the classification of simple and complex cells. Vision Res.2002.Apr;42.(8.):1017.-33. *42*, 1017-1033.

46. Michael,C.R. (1968). Receptive fields of single optic nerve fibers in a mammal with an all-cone retina. 3. Opponent color units. J.Neurophysiol. *31*, 268-282.

47. Mooney,R.D., Klein,B.G., and Rhoades,R.W. (1985). Correlations between the structural and functional characteristics of neurons in the superficial laminae and the hamster's superior colliculus. Journal of Neuroscience *5*, 2989-3009.

48. Naumann E.A. and Engert F. Using G-CaMP 1.6 to Monitor Visually-Evoked Synaptic Activity in Tectal Neurons *in vivo*. 2005.
Ref Type: Thesis/Dissertation

49. Neuhauss,S.C. (2003). Behavioral genetic approaches to visual system development and function in zebrafish. Journal of Neurobiology *54*, 148-160.

50. Neuhauss,S.C., Biehlmaier,O., Seeliger,M.W., Das,T., Kohler,K., Harris,W.A., and Baier,H. (1999). Genetic disorders of vision revealed by a behavioral screen of 400 essential loci in zebrafish. Journal of Neuroscience *19*, 8603-8615.

51. Niell,C.M., Meyer,M.P., and Smith,S.J. (2004). In vivo imaging of synapse formation on a growing dendritic arbor. Nat.Neurosci. *7*, 254-260.

52. Niell,C.M. and Smith,S.J. (2005). Functional imaging reveals rapid development of visual response properties in the zebrafish tectum. Neuron *45*, 941-951.

53. Orger,M.B., Gahtan,E., Muto,A., Page-McCaw,P., Smear,M.C., and Baier,H. (2004). Behavioral screening assays in zebrafish. Methods Cell Biol.2004.;77.:53.-68. *77*, 53-68.

54. Pinter,R.B. and Harris,L.R. (1981). Temporal and spatial response characteristics of the cat superior colliculus. Brain Research *207*, 73-94.

55. Rae,J., Cooper,K., Gates,P., and Watsky,M. (1991). Low access resistance perforated patch recordings using amphotericin B. J.Neurosci Methods *37*, 15-26.

56. Reich,D.S., Victor,J.D., Knight,B.W., Ozaki,T., and Kaplan,E. (1997). Response variability and timing precision of neuronal spike trains in vivo. J.Neurophysiol. *77*, 2836-2841.

57. Reid,R.C., Soodak,R.E., and Shapley,R.M. (1991). Directional selectivity and spatiotemporal structure of receptive fields of simple cells in cat striate cortex. J.Neurophysiol. *66*, 505-529.

58. Reid,R.C., Victor,J.D., and Shapley,R.M. (1997). The use of m-sequences in the analysis of visual neurons: linear receptive field properties. Visual Neuroscience *14*, 1015-1027.

59. Reinagel,P. and Reid,R.C. (2000). Temporal coding of visual information in the thalamus. J.Neurosci.2000.Jul.15.;20.(14):5392.-400. *20*, 5392-5400.

60. Rieke,F. and Baylor,D.A. (1998). Origin of reproducibility in the responses of retinal rods to single photons. Biophysical Journal *75*, 1836-1857.

61. Ringach,D.L. (2004). Mapping receptive fields in primary visual cortex. J.Physiol 2004.Aug.1;558.(Pt.3):717.-28.Epub.2004.May.21. *558*, 717-728.

62. Ringach,D.L., Sapiro,G., and Shapley,R. (1997). A subspace reverse-correlation technique for the study of visual neurons. Vision Research *37*, 2455-2464.

63. Rinner,O., Makhankov,Y.V., Biehlmaier,O., and Neuhauss,S.C. (2005a). Knockdown of cone-specific kinase GRK7 in larval zebrafish leads to impaired cone response recovery and delayed dark adaptation. Neuron 2005.Jul.21;47.(2):231.-42. *47*, 231-242.

64. Rinner,O., Rick,J.M., and Neuhauss,S.C. (2005b). Contrast sensitivity, spatial and temporal tuning of the larval zebrafish optokinetic response. Invest Ophthalmol.Vis.Sci.2005.Jan.;46.(1):137.-42. *46*, 137-142.

65. Roeser,T. and Baier,H. (2003). Visuomotor Behaviors in Larval Zebrafish after GFP-Guided Laser Ablation of the Optic Tectum. Journal of Neuroscience *23*, 3726-3734.

66. Sajovic,P. and Levinthal,C. (1982a). Visual cells of zebrafish optic tectum: mapping with small spots. Neuroscience *7*, 2407-2426.

67. Sajovic,P. and Levinthal,C. (1982b). Visual response properties of zebrafish tectal cells. Neuroscience *7*, 2427-2440.

68. Sajovic,P. and Levinthal,C. (1983). Inhibitory mechanism in zebrafish optic tectum: visual response properties of tectal cells altered by picrotoxin and bicuculline. Brain Research *271*, 227-240.

69. Saul,A.B. and Humphrey,A.L. (1990). Spatial and temporal response properties of lagged and nonlagged cells in cat lateral geniculate nucleus. J.Neurophysiol. *64*, 206-224.

70. Shadlen,M.N. and Newsome,W.T. (1998). The variable discharge of cortical neurons: implications for connectivity, computation, and information coding. Journal of Neuroscience *18*, 3870-3896.

71. Touryan,J., Felsen,G., and Dan,Y. (2005). Spatial structure of complex cell receptive fields measured with natural images. Neuron *45*, 781-791.

72. Trowe,T., Klostermann,S., Baier,H., Granato,M., Crawford,A.D., Grunewald,B., Hoffmann,H., Karlstrom,R.O., Meyer,S.U., Muller,B., Richter,S., Nusslein-Volhard,C., and Bonhoeffer,F. (1996). Mutations disrupting the ordering and topographic mapping of axons in the retinotectal projection of the zebrafish, Danio rerio. Development *123*, 439-450.

73. Van Hooser,S.D., Heimel,J.A., and Nelson,S.B. (2003). Receptive field properties and laminar organization of lateral geniculate nucleus in the gray squirrel (Sciurus carolinensis). J.Neurophysiol. *90*, 3398-3418.

74. Vislay-Melzer (2005). Spatio-temporal specificity of neuronal activity directs the modification of receptive fields in the developing retinotectal system.

75. Vogel,G. (2000). Zebrafish earns its stripes in genetic screens [news]. Science *288*, 1160-1161.

76. Westerfield,M. (1993). The Zebrafish Book. Eugene: University of Oregon Press.).

77. Worgotter,F., Suder,K., and Funke,K. (1999). The dynamic spatio-temporal behavior of visual responses in thalamus and cortex. Restor.Neurol.Neurosci. *15*, 137-152.

78. Wullimann,M.F., Rupp,B., and Reichert,H. (1996). Neuroanatomy of the Zebrafish brain- A topological Atlas. Birkhaeuser).

79. Zhang,L.I., Tao,H.W., Holt,C.E., Harris,W.A., and Poo,M.M. (1998). A critical window for cooperation and competition among developing retinotectal synapses. Nature *395*, 37-44.

PUBLICATIONS BETTINA REITER

Reiter, B and Grothe, B: "Tonotopy and morphology of the inferior colliculus in wildtype and wnt-1 mutant mice", abstract submission for ARO meeting 2002, Florida

Reiter, B, Kampff, AR and Engert, F: "Receptive fields and motion detection of tectum cells in zebrafish larvae", poster presentation at FENS 2004, Lisbon Portugal

Ramdya, P, Reiter, B and Engert, F: "Reverse correlation of rapid calcium signals in the zebrafish optic tectum *in vivo"*, in submission

Reiter, B, Kampff, AR and Engert, F: "Temporal and spatial receptive field characteristics of tectal neurons in zebrafish larvae", publication of this thesis, in preparation.

Acknowledgements:

I would like to than Tobias Bonhoeffer for accepting me as his PhD candidate and helping me make the connection with Florian Engert.

I want to thank Florian! Without his endless patience and encouraging enthusiasm this thesis would never have been accomplished. He also gave me the opportunity to gain intense insight into the field of lab management. Most importantly I am thankful that we could uphold such a wonderful friendship throughout these years!

Thanks to the members of my committee at Harvard, John Dowling, Markus Meister, and Venky Murthy for their time and advices, and thanks to the committee at the MPI in Munich, Tobias Bonhoeffer, Benedikt Grothe, Mark Hübener, and Rainer Uhl who agreed to participate in the evaluation of my PhD.

I thank all the members of the Engert lab for being good friends and for creating such a fun environment. Specifically, I want to thank Adam Kampff who wrote endless versions of acquisition and analysis software for me and the lab in general and was always helpful with ideas and advice.

I thank the whole MCB community for making my stay here at Harvard so pleasant and for creating an overall caring work environment, especially the students who are G5s this year who were so welcoming and "adopted" me into their class.

I thank my good friends Nicola, Lorena and Kate who were always there for me.

Last but not least I thank my family who encouraged me along the way and made all of this possible.

Ehrenwoertliche Vesicherung:

Ich vesichere heiermit ehrenwoertlich, dass meine Dissertation mit dem Titel **"Temporal and spatial receptive field characteristics of tectal neurons in zebrafish larvae"** von mir selbstständig und ohne unerlaubte Hilfe angefertigt ist. Woertlich oder inhaltlich uebernommene Stellen sind als solche gekennzeichnet.

Erklaerung:

Hiermit erklaere ich, dass ich mich nicht anderwertig einer Doktorpruefung ohne Erfolg unterzogen habe.

CURRICULUM VITAE   **BETTINA REITER**

Address: Bettina Reiter
                Biolabs 2073
                Harvard University
                16 Divinity Ave
                Cambridge, MA 02138

e-mail: tini@mcb.haravrd.edu
phone: (617) 384 9773 (office)
                (6170 642 4651 (cell phone)
                (617) 384 9600 (fax)

Date of birth: June 1st, 1976
Place of birth: Kronberg, Germany
Nationality: German
Marital state: single

1982-1986	Elementary school in Schlossborn
1986-1992	High school in Königstein, Germany
1992-1993	High school in Merida, Venezuela
1993-1995	High school in Kelkheim, Germany Abitur (high-school diploma): June 1995
1995-1997	Study of basic Biology at the Philipps University of Marburg, Germany
1997-2000	Study of Neurobiology at the Ludwig-Maximilians University of Munich, Germany
2000-2001	Diploma thesis with Dr. Benedikt Grothe on "Morphology and Physiology of midbrain neurons in a wnt-1 overexpressing mouse" at the MPI of Neurobiology in Martinsried, Germany
2002-pesent	PhD project with Dr. Florian Engert on "Receptive fields and motion detection in the visual System of zebrafish larvae" at Harvard University, Cambridge, MA